Dopamine Negatively Modulates the NCA Ion Channels in *C. elegans*

Irini Topalidou[*], Kirsten Cooper[1], Laura Pereira[†], and Michael Ailion[*]

Department of Biochemistry, University of Washington, Seattle, WA, USA

[†]Department of Biological Sciences, Howard Hughes Medical Institute, Columbia University, New York, NY, USA

[1]Current address: Fred Hutchinson Cancer Research Center, Seattle, WA, USA

[*]Corresponding authors

Email: it2117@uw.edu (IT), mailion@uw.edu (MA)

Short title: NCA modulation by GRK-2 and dopamine

Abstract

The NALCN/NCA ion channel is a cation channel related to voltage-gated sodium and calcium channels. NALCN has been reported to be a sodium leak channel with a conserved role in establishing neuronal resting membrane potential, but its precise cellular role and regulation are unclear. The *Caenorhabditis elegans* orthologs of NALCN, NCA-1 and NCA-2, act in premotor interneurons to regulate motor circuit activity that sustains locomotion. Recently we found that NCA-1 and NCA-2 are activated by a signal transduction pathway acting downstream of the heterotrimeric G protein G_q and the small GTPase Rho. Through a forward genetic screen, here we identify the GPCR kinase GRK-2 as a new player affecting signaling through the G_q-Rho-NCA pathway. Using structure-function analysis, we find that the GPCR phosphorylation and membrane association domains of GRK-2 are required for its function. Genetic epistasis experiments suggest that GRK-2 acts on the D2-like dopamine receptor DOP-3 to inhibit G_o signaling and positively modulate NCA-1 and NCA-2 activity. Through cell-specific rescuing experiments, we find that GRK-2 and DOP-3 act in premotor interneurons to modulate NCA channel function. Finally, we demonstrate that dopamine, through DOP-3, negatively regulates NCA activity. Thus, this study identifies a pathway by which dopamine modulates the activity of the NCA channels.

Author summary

Dopamine is a neurotransmitter that acts in the brain by binding seven transmembrane receptors that are coupled to heterotrimeric GTP-binding proteins (G proteins). Neuronal G proteins often function by modulating ion channels that control membrane excitability. Here we identify a molecular cascade downstream of dopamine in the nematode *C. elegans* that involves activation of the dopamine receptor DOP-3, activation of the G protein GOA-1, and inactivation of the NCA-1 and NCA-2 ion channels. We also identify a G protein-coupled receptor kinase (GRK-2) that inactivates the dopamine receptor DOP-3, thus leading to inactivation of GOA-1 and activation of the NCA channels. Thus, this study connects dopamine signaling to activity of the NCA channels through G protein signaling pathways.

45 **Introduction**

46 Heterotrimeric G proteins modulate neuronal activity in response to experience or environmental
47 changes. G_q is one of the four types of heterotrimeric G protein alpha subunits [1] and is a positive
48 regulator of neuronal activity and synaptic transmission [2–4]. In the canonical G_q pathway, G_q activates
49 phospholipase Cβ (PLCβ) to cleave the lipid phosphatidylinositol 4,5-bisphosphate (PIP2) into diacylglycerol
50 (DAG) and inositol trisphosphate (IP3), which act as second messengers. In a second major G_q signal
51 transduction pathway, G_q directly binds and activates Rho guanine nucleotide exchange factors (GEFs),
52 activators of the small GTPase Rho [5–8]. Rho regulates many biological functions including actin
53 cytoskeleton dynamics and neuronal development, but less is known about Rho function in mature
54 neurons. In *C. elegans*, Rho has been reported to stimulate synaptic transmission through multiple
55 pathways [9–11]. We recently identified the *C. elegans* orthologs of the NALCN ion channel, NCA-1 and
56 NCA-2, as downstream targets of a G_q-Rho signaling pathway [12]. We aim to understand the mechanism
57 of activation of this pathway.

58 The NALCN/NCA ion channel is a nonselective cation channel that is a member of the voltage-gated
59 sodium and calcium channel family [13–15]. The NALCN channel was proposed to be the major contributor
60 to the sodium leak current that helps set the resting membrane potential of neurons [16], though there is
61 controversy whether NALCN is indeed a sodium leak channel [17–19]. In humans, mutations in *NALCN* or
62 its accessory subunit *UNC80* have been associated with a number of neurological symptoms, including
63 cognitive and developmental delay [20–33]. In other organisms, mutations in NALCN/NCA or its accessory
64 subunits lead to defects in rhythmic behaviors [16,34–42]. Specifically in *C. elegans*, the NCA channels act
65 in premotor interneurons where they regulate persistent motor circuit activity that sustains locomotion
66 [43]. In addition to the G_q-Rho pathway described above, two other mechanisms have been reported to
67 regulate the activity of the NALCN channel: a G protein-independent activation of NALCN by G protein-

68 coupled receptors [44,45] and a G protein-dependent regulation by extracellular Ca^{2+} [46]. Here we
69 identify a molecular cascade downstream of dopamine in the nematode *C. elegans* that involves the D2-
70 like dopamine receptor DOP-3 and the G protein-coupled receptor kinase GRK-2 to modulate activity of
71 the NCA-1 and NCA-2 ion channels.

72 G protein-coupled receptor kinases (GRKs) are protein kinases that phosphorylate and desensitize G
73 protein-coupled receptors (GPCRs). Mammalian GRKs have been divided into three groups based on their
74 sequences and function: 1) GRK1 and GRK7, 2) GRK2 and GRK3, and 3) GRK4, GRK5 and GRK6 [47]. *C.*
75 *elegans* has two GRKs: GRK-1 and GRK-2, orthologs of the GRK4/5/6 and GRK2/3 families respectively [48].
76 Mammalian GRK2 is ubiquitously expressed [49,50] and GRK2 knock-out mice die as embryos [51]. In *C.*
77 *elegans*, *grk-2* is expressed in the nervous system and required for normal chemosensation [52] and egg-
78 laying [53]. In this study, we find that *C. elegans grk-2* mutants have locomotion defects due to decreased
79 G_q signaling. We identify the D2-like dopamine receptor DOP-3 as the putative GRK-2 target and find that
80 GRK-2 acts through DOP-3 to inhibit G_o signaling. This in turn leads to activation of the NCA channels
81 through the G_q-Rho signaling pathway. We also find that GRK-2 and DOP-3 exert their effect by acting in
82 the premotor interneurons, where the NCA channels also act to regulate persistent motor neuron activity
83 [43].

84 The D2-like receptors are GPCRs that couple to members of the inhibitory $G_{i/o}$ family [54]. In
85 mammals, GRK2 has been connected to the regulation of D2-type dopamine receptors, but the reported
86 results are based mainly on effects of GRK2 overexpression in heterologous expression systems [55–59].
87 The results reported here provide a direct connection between GRK-2 and D2-type receptor signaling in a
88 behaviorally relevant *in vivo* system. In *C. elegans,* dopamine, through *dop-3*, causes the slowing of the
89 worm's locomotion rate on food [60]; DOP-3 signals through G_o to inhibit locomotion [61]. Here we find
90 that dopamine, through activation of DOP-3, negatively modulates the activity of the NCA channels. This

91 suggests a model in which dopamine signaling negatively regulates NCA channel activity and sustained
92 locomotion through G protein signaling acting in premotor interneurons.
93
94 ## Results
95
96 **The G protein-coupled receptor kinase GRK-2 promotes G_q signaling**
97 To identify regulators of G_q signaling, we performed a forward genetic screen in the
98 nematode *C. elegans* for suppressors of the activated G_q mutant *egl-30*(*tg26)* [62,63]. The *egl-30(tg26)*
99 mutant is hyperactive and has a tightly coiled "loopy" posture (Fig 1A and B). These phenotypes were
100 suppressed by the *yak18* mutation isolated in our screen (Fig 1A). When outcrossed away from the *egl-*
101 *30(tg26)* mutation, *yak-18* mutant animals are shorter than wild type animals, have slow locomotion (Fig
102 1C, Right), and are egg-laying defective.
103 We mapped *yak18* to the left arm of Chromosome III and cloned it by whole-genome sequencing and a
104 complementation test with the deletion allele *grk-2(gk268*) (see Methods). *yak18* is a G to A transition
105 mutation in the W02B3.2 *(grk-2*) ORF that leads to the missense mutation G379E in the kinase domain of
106 GRK-2. GRK-2 is a serine/threonine protein kinase orthologous to the human GPCR kinases GRK2 and GRK3
107 [52]. The deletion allele *grk-2(gk268)* also suppresses the loopy posture and hyperactive locomotion of
108 activated G_q (Fig 1A and B) and causes defects in locomotion, egg-laying, and body-size similar to *grk-*
109 *2(yak18)* (Fig 1C Left, S1A and S1B). We also found that *grk-2* mutant animals are defective in swimming
110 (Fig S2), a locomotion behavior that has distinct kinematics to crawling [64]. Additionally, *grk-2* mutants
111 restrict their movements to a limited region of a bacterial lawn, whereas wild-type animals explore the
112 entire lawn (Fig S1C).
113 Our data suggest that GRK-2 regulates locomotion and is a positive regulator of G_q signaling. The
114 standard model of GRK action is that GPCR phosphorylation by GRK triggers GPCR binding to the inhibitory
115 protein beta-arrestin; binding of arrestin blocks GPCR signaling and mediates receptor internalization [65].

116 We tested whether loss of arrestin causes defects similar to loss of *grk-2* by using a deletion allele in *arr-1,*
117 the only *C. elegans* beta-arrestin homolog. We found that *arr-1(ok401)* mutant animals do not have slow
118 locomotion (Fig S3A). To test whether an *arr-1* mutation suppresses activated G_q, we constructed an *egl-*
119 *30(tg26)* mutant strain carrying an *arr-1* mutation in trans to a closely linked RFP marker (that is, an *egl-*
120 *30(tg26); arr-1/*RFP strain). Surprisingly, this strain segregated few viable non-red animals, suggesting that
121 *egl-30(tg26); arr-1* double mutants are subviable. The few *egl-30(tg26); arr-1* viable animals looked similar
122 to the *egl-30(tg26)* single mutant (Fig S3B), but died as young adults. These results suggest that GRK-2 acts
123 independently of arrestin to regulate locomotion rate and G_q signaling.

124 In addition to phosphorylation of GPCRs, mammalian GRK2 can also regulate signaling in a
125 phosphorylation-independent manner [66,67]. Thus, we tested whether the kinase activity of GRK-2 is
126 required for proper locomotion and G_q signaling by assaying whether a kinase-dead GRK-2[K220R] mutant
127 [48,68] is capable of rescuing the *grk-2(gk268)* and *egl-30(tg26); grk-2(gk268)* mutants. Wild type GRK-2
128 rescued the locomotion defect of *grk-2(gk268)* mutants (Fig 1C, Left), but the kinase dead GRK-2[K220R],
129 although it was properly expressed (Fig 2G), did not rescue either the locomotion defect or the
130 suppression of activated G_q (Fig 1C and D). We conclude that GRK-2 acts as a kinase to regulate locomotion
131 rate and G_q signaling.

132

133 **GPCR-phosphorylation and membrane association domains of GRK-2 are required for its function in**
134 **locomotion**

135 To examine whether GRK-2 acts as a GPCR kinase to control locomotion, we took a structure-function
136 approach (Fig 2A). We took advantage of previously-described mutations that disrupt specific activities of
137 GRK-2, but do not disrupt GRK-2 protein expression or stability [48]. These mutations all affect conserved
138 residues in well-characterized domains of GRK-2 [48].

139 Although GRKs act as kinases for activated GPCRs, mammalian GRKs have been shown to interact with
140 and phosphorylate other molecules as well [66,67]. Therefore, although the kinase activity of GRK-2 is
141 required for locomotion, it is possible that the relevant targets are proteins other than GPCRs. To examine
142 whether phosphorylation of GPCRs is required for GRK-2 function in locomotion, we expressed GRK-2 with
143 mutations (D3K, L4K, V7A/L8A, and D10A) that have been shown to reduce mammalian GRK2
144 phosphorylation of GPCRs, but that do not affect phosphorylation of other targets [69]. These N-terminal
145 residues of mammalian GRKs form an amphipathic α-helix that contributes specifically to GPCR
146 phosphorylation [70–74]. *grk-2(gk268)* mutants expressing any of these mutant GRK-2 constructs had slow
147 locomotion like *grk-2(gk268)* (Fig 2B, 2C and 2G), indicating that GPCR phosphorylation is required for
148 GRK-2 function in locomotion *in vivo*.

149 In mammalian GRKs, interaction of the N-terminal region with the kinase domain stabilizes a closed
150 and more active conformation of the enzyme, important for phosphorylation of GPCRs and other
151 substrates [70–72]. Specifically, mutation of mammalian GRK1 Arg191 disrupted phosphorylation of target
152 substrates in addition to GPCRs, suggesting that this residue is critical for conformational changes
153 important for GRK function as a kinase [71]. To determine whether the analogous residue in GRK-2 is
154 required for its function in locomotion, we expressed GRK-2[R195A] in *grk-2(gk268)* mutants. GRK-
155 2[R195A] did not rescue the *grk-2(gk268)* locomotion phenotype (Fig 2D and 2G), further supporting the
156 model that GRK-2 acts as a GPCR kinase to regulate locomotion.

157 The RH (Regulator of G protein Signaling Homology) domain of mammalian GRK2 (Fig 2A) does not act
158 like other RGS domains as an accelerator of the intrinsic GTPase activity of the G_q subunit, but instead
159 interacts with G_q and participates in the uncoupling of GPCRs linked to G_q via a phosphorylation-
160 independent mechanism [67,74]. To examine whether the G_q-binding residues of the RH domain are
161 needed for GRK-2 function in locomotion, we expressed GRK-2[R106A], Y109I, and D110A that correspond
162 to mutations previously shown to disrupt mammalian GRK2 binding to $G_{q/11}$ [75]. All three mutant GRK-2

163 constructs rescued the slow locomotion defect of *grk-2(gk268)* (Fig 2E and 2G). These results suggest that
164 GRK-2 binding to G_q and phosphorylation-independent desensitization of GPCR signaling are not required
165 for GRK-2 function in locomotion.

166 The pleckstrin homology (PH) domain of mammalian GRK2 (Fig 2A) mediates interactions of GRK2 with
167 membrane phospholipids and Gβγ subunits [67,76–78]. To examine whether these activities are required
168 for GRK-2 function in locomotion, we expressed GRK-2[K567E] that disrupts phospholipid binding [79] and
169 GRK-2[R587Q] that disrupts binding to Gβγ [79]. Neither of these GRK-2 mutants rescued the locomotion
170 defect of the *grk-2(gk268)* mutant (Fig 2F and 2G), suggesting that both phospholipid and Gβγ binding
171 through the PH domain of GRK-2 are required for GRK-2 function in locomotion.

172

173 **GRK-2 acts in head acetylcholine neurons to control locomotion and G_q signaling**

174 GRK-2 is broadly expressed in body and head neurons [52]. To determine where GRK-2 acts to control
175 locomotion, we expressed the *grk-2* cDNA under the control of neuron-specific promoters. Expression
176 of *grk-2* under the pan-neuronal (*Prab-3*) or acetylcholine neuron (*Punc-17*) promoters fully rescued *grk-*
177 *2(gk268)* mutant locomotion (Fig 3A). Interestingly, expression in ventral cord acetylcholine motor neurons
178 (*Pacr-2*) did not rescue the locomotion phenotype, but expression driven by an *unc-17* promoter derivative
179 that is expressed mainly in the head acetylcholine neurons (*Punc-17H* [80,81]) rescued the locomotion
180 phenotype (Fig 3A). Additionally, expression driven in a number of interneurons and head motorneurons
181 by the *glr-1* promoter did not rescue (Fig 3A). To exclude the possibility that the described role of GRK-2 in
182 chemosensation [52] contributes to the slow locomotion phenotype of *grk-2* mutants, we expressed *grk-2*
183 under ciliated sensory neuron promoters (*Pxbx-1* and *Posm-6*). Expression of *grk-2* in ciliated sensory
184 neurons did not rescue the slow locomotion of *grk-2* mutants (Fig 3A). We conclude that *grk-2* acts in head
185 acetylcholine neurons to regulate locomotion.

186 To determine if *grk-2* also acts in head acetylcholine neurons to regulate G_q signaling, we expressed
187 the *grk-2* cDNA in the head acetylcholine neurons of *egl-30(tg26); grk-2* double mutants. Expression in
188 head acetylcholine neurons reversed the *grk-2* suppression of the loopy posture and hyperactive
189 locomotion of activated G_q – that is, the *egl-30(tg26); grk-2* double mutants expressing *grk-2* cDNA in the
190 head acetylcholine neurons resemble the activated G_q single mutant (Fig 3B and C). These results suggest
191 that *grk-2* acts in head acetylcholine neurons to positively regulate G_q signaling.
192 To confirm that *grk-2* is expressed in the head acetylcholine neurons, we coexpressed tagRFP fused to
193 GRK-2 driven by the *grk-2* promoter (*grk-2*::tagRFP) and GFP driven by the head acetylcholine neuron
194 promoter (*Punc-17H*::GFP). We observed that *grk-2*::tagRFP is expressed broadly in head neurons and
195 colocalizes with GFP in several head acetylcholine neurons (Fig 3D). We conclude that GRK-2 is expressed
196 in head acetylcholine neurons to regulate locomotion and G_q signaling.
197
198 **GRK-2 acts upstream of G_o to regulate locomotion**
199 Our results suggest that GRK-2 acts as a GPCR kinase to regulate locomotion. If GRK-2 were a kinase for
200 a GPCR coupled to G_q (EGL-30 in *C. elegans*) then we would expect GRK-2 to negatively regulate G_q, which
201 does not agree with our data. Alternatively, GRK-2 could be a kinase for a GPCR coupled to G_o (GOA-1 in *C.*
202 *elegans*). The *C. elegans* G_q and G_o pathways act in opposite ways to regulate locomotion by controlling
203 acetylcholine release [82]. EGL-30 is a positive regulator of acetylcholine release whereas GOA-1 negatively
204 regulates the EGL-30 pathway through activation of the RGS protein EAT-16 and the diacylglycerol kinase
205 DGK-1. *egl-30* loss-of-function mutants are immobile whereas *egl-30* gain-of-function mutants are
206 hyperactive and have a loopy posture [83,84]. *goa-1* and *eat-16* mutants have locomotion phenotypes
207 opposite those of *egl-30*; they are hyperactive and have a loopy posture [85–87]. *dgk-1* loss-of-function
208 mutants are hyperactive but do not have a loopy posture [88]. To test whether GRK-2 acts on a G_o-coupled
209 GPCR, we examined whether *goa-1* mutations suppress *grk-2* mutants. We found that the *goa-1; grk-2*

210 double mutant is hyperactive and has a loopy posture like the *goa-1* single mutant (Fig S4A, S4C and S4D),
211 indicating that GRK-2 acts upstream of *goa-1*. This result suggests that GRK-2 could be acting on GPCR(s)
212 coupled to GOA-1.

213 To further dissect the GRK-2 pathway, we examined whether *grk-2* mutations suppress the hyperactive
214 phenotypes of *eat-16* and *dgk-1* mutants. The *eat-16; grk-2* double mutant is hyperactive and has a loopy
215 posture like the *eat-16* single mutant (Fig S4A, S4C and S4D) indicating that *eat-16*, like *goa-1*, acts
216 downstream of GRK-2. By contrast, the *grk-2; dgk-1* double mutant is similar to *grk-2* (Fig S4B). Expression
217 of the kinase dead GRK-2[K220R] in *grk-2; dgk-1* mutants does not restore *dgk-1* hyperactive locomotion
218 (Fig S4E). In addition, expression of GRK-2 under a head acetylcholine neuron promoter in *grk-2; dgk-1*
219 mutants restores *dgk-1* hyperactive locomotion (Fig S4F). Thus, GRK-2 regulation of the locomotion rate,
220 G_q signaling, and DAG signaling all depend on the GRK-2 kinase activity and a function of GRK-2 in head
221 acetylcholine neurons.

222

223 **GRK-2 regulates the DOP-3 dopamine receptor**

224 In a search for potential G_o-coupled GPCR targets for GRK-2, we considered the G_o-coupled D2-like
225 dopamine receptor DOP-3. In *C. elegans*, dopamine is required for the "basal slowing response", a
226 behavior in which wild type animals slow down when on a bacterial lawn [89]. This behavior is mediated by
227 the mechanosensory activation of dopamine neurons caused by physical contact of the worm body with
228 bacteria. *cat-2* mutants that are deficient in dopamine biosynthesis [90] or *dop-3* mutants that lack the D2-
229 like dopamine receptor DOP-3, are defective in basal slowing [61,89]. DOP-3 has been proposed to act
230 through G_o in ventral cord acetylcholine motor neurons to decrease acetylcholine release and promote the
231 basal slowing response [61].

232 If *grk-2* acts in the dopamine pathway to mediate proper locomotion, possibly by phosphorylating and
233 inactivating DOP-3, then mutations in *dop-3* and *cat-2* should suppress the *grk-2* locomotion phenotype.

234 Indeed, the *grk*-2 mutant slow locomotion phenotype was suppressed by mutations in *dop-3* and *cat-2* (Fig
235 4A). A *dop-3* mutation also suppressed the swimming defect of the *grk-2* mutant (Fig S2). In addition, the
236 *dop-3* and *cat-2* mutations reversed the *grk-2* suppression of the loopy posture and hyperactive
237 locomotion of activated G_q – that is, the triple mutants resemble the activated G_q single mutant (Fig 4B-E
238 and Fig S5). These results suggest that GRK-2 acts in the dopamine pathway to regulate locomotion and G_q
239 signaling by negatively regulating the D2-like dopamine receptor DOP-3.

240 Our results suggest that GRK-2 acts in head acetylcholine neurons to regulate locomotion. To test if
241 DOP-3 acts in the same neurons as GRK-2, we expressed the *dop-3* cDNA under a pan-neuronal promoter
242 (*Prab-3*), an acetylcholine neuron promoter (*Punc-17*), a head acetylcholine neuron promoter (*Punc-17H*),
243 and an acetylcholine motor neuron promoter (*Pacr-2*) in the *grk-2; dop-3* double mutant. Expression
244 driven by the pan-neuronal, acetylcholine neuron, and head acetylcholine neuron promoters reversed the
245 *dop-3* suppression of the slow locomotion of *grk-2(gk268)* mutant animals – that is, *grk-2; dop-3* mutants
246 expressing *dop-3* cDNA by these three promoters resemble the *grk-2* mutant (Fig S6A). By contrast,
247 expression of the *dop-3* cDNA by an acetylcholine ventral cord motor neuron promoter did not reverse the
248 *grk-2; dop-3* locomotion phenotype (Fig S6A) or the hyperactive locomotion and loopy posture of *egl-*
249 *30(tg26); grk-2; dop-3* mutant animals (Fig S6C-E). We conclude that *dop-3*, like *grk-2*, acts in head
250 acetylcholine neurons, consistent with the model that GRK-2 acts directly on DOP-3. Moreover, *dop-3*
251 expression under the *grk-2* promoter reversed the *dop-3* suppression of the slow locomotion of *grk-2*
252 mutants (Figure S7A), supporting the idea that GRK-2 and DOP-3 act in the same neurons.

253 We observed that *grk-2; dop-3* and *cat-2; grk-2* double mutant animals still retain some of the
254 characteristic *grk-2* phenotypes: the animals have shorter bodies and are egg-laying defective. In addition,
255 *grk-2* mutants do not fully explore a bacterial lawn and this behavior remains in the *grk-2; dop-3* double
256 mutant (Fig S1C). Thus, GRK-2 has additional neuronal functions that do not depend on *dop-3*.

257 The D1-like dopamine receptor DOP-1 has been shown to act antagonistically to DOP-3 to regulate the
258 basal slowing response: *dop-1* mutations suppress the *dop-3* basal slowing phenotype [61]. By contrast, we
259 found that DOP-1 is not involved in the GRK-2 and DOP-3 pathway that regulates locomotion rate because
260 *dop-1* mutations do not affect the locomotion rate of the *grk-2; dop-3* double mutant (Fig S6B). Thus, the
261 role of DOP-3 in GRK-2-regulated locomotion is independent of its role in the basal slowing response.
262 Exposure of *C. elegans* to exogenous dopamine causes DOP-3-dependent paralysis — *dop-3* mutants
263 are significantly resistant to the paralytic effects of exogenous dopamine [61]. If GRK-2 negatively
264 regulates DOP-3, then *grk-2* mutants might be hypersensitive to dopamine due to increased DOP-3
265 activity. Indeed, we found that *grk-2* mutants are hypersensitive to dopamine and this hypersensitivity
266 depends on *dop-3* (Fig 4F).
267 In an effort to dissect the molecular mechanism by which *grk-2* regulates DOP-3 activity, we
268 expressed GFP-tagged DOP-3 under the *grk-2* promoter in *dop-3* and *grk-2; dop-3* mutant animals and
269 examined the levels of expression of DOP-3::GFP both by Western and by fluorescence microscopy (Fig
270 S7). Although *Pgrk-2*::DOP-3::GFP fully reversed the *dop-3* suppression of the slow locomotion of *grk-2*
271 mutants (Fig S7A), we did not observe any difference in the level of DOP-3 expression in a *grk-2* mutant
272 (Fig S7B-D) nor did we observe any obvious change in the subcellular localization of DOP-3::GFP in a *grk-2*
273 mutant (Fig S7C). However, one caveat is that we do not have the resolution to distinguish between DOP-3
274 localization on the plasma membrane or in an intracellular compartment.
275
276 **GRK-2 is a positive modulator of NCA-1 and NCA-2 channel activity**
277 In addition to genes within the canonical G_q-PLCβ pathway, our screen for suppressors of activated G_q
278 also identified the Trio RhoGEF (UNC-73 in *C. elegans*) as a new direct G_q effector [8]. Recently, we
279 identified the cation channels NCA-1 and NCA-2 as downstream targets of this G_q-Rho pathway.
280 Specifically, we found that mutations in genes that encode accessory subunits of the NCA channels (*unc-*

281 *79, unc-80*) or in the NCA channels per se (*nca-1; nca-2*) suppress the neuronal phenotypes of activated G_q
282 and activated Rho [12]. Moreover, mutations in the Rho-NCA pathway suppress the loopy posture of the
283 activated G_q mutant more strongly than do mutations in the canonical PLCβ pathway [12]. Like mutations
284 in the Rho-NCA pathway, *grk-2* mutants also strongly suppress the loopy posture of an activated G_q mutant
285 (Fig 1A, 4D and 4E), suggesting that *grk-2* may affect signaling through the Rho-NCA pathway.

286 To further examine whether *grk-2* affects Rho-NCA signaling, we built double mutants of *grk-2* with an
287 activated Rho mutant (G14V), referred to here as Rho*, expressed in acetylcholine neurons. Rho* has a
288 loopy posture and slow locomotion and a *grk-2* mutation partially suppresses these phenotypes (Fig 5A
289 and 5B), consistent with *grk-2* affecting signaling through the Rho-NCA pathway.

290 We also built double mutants of *grk-2* and a dominant activating mutation in the NCA-1 channel gene,
291 *nca-1(ox352),* referred to here as Nca* [12,24]. Like Rho*, Nca* mutants have a loopy posture and slow
292 locomotion. However, *grk-2* mutants do not suppress either of these phenotypes because Nca*; *grk-2*
293 double mutants behave identically to Nca* mutants (Fig 5C and 5D). This suggests that *grk-2* acts upstream
294 of NCA.

295 *C. elegans* has two proteins that encode pore-forming subunits of NCA channels, NCA-1 and NCA-2.
296 Mutations that disrupt both NCA-1 and NCA-2 channel activity cause a characteristic "fainter" phenotype
297 in which worms suddenly arrest their locomotion and acquire a straightened posture [35]. Our genetic
298 experiments indicate that GRK-2 affects Rho-NCA signaling, but *grk-2* mutants are not fainters. Given that
299 *grk-2* partially suppresses Rho*, we hypothesized that GRK-2 is not absolutely required for Rho-NCA
300 signaling, but provides modulatory input. To test this hypothesis, we built double mutants between *grk-2*
301 and *nlf-1*, which is partially required for localization of the NCA-1 and NCA-2 channels and has a weak
302 fainter mutant phenotype [12,91]. A *grk-2* mutation strongly enhanced the weak fainter phenotype of an
303 *nlf-1* mutant so that the double mutants resembled the stronger fainter mutants that completely abolish
304 NCA-1 and NCA-2 channel activity (Fig 6A and 6B). Moreover, double mutants between *grk-2* and the

305 RhoGEF Trio *unc-73* were also strong fainters, supporting the hypothesis that GRK-2 modulates the Rho-
306 NCA pathway (Fig 6C). By contrast, double mutants between *grk-2* and the *egl-8* PLCβ do not have a
307 fainter phenotype (Fig 6C). These results suggest that GRK-2 is a positive modulator of NCA-1 and NCA-2
308 channel activity.

309 If GRK-2 modulates the NCA channels by acting as a negative regulator of G_o then we would expect
310 that mutations in other proteins that act as negative regulators of G_o might enhance the fainter phenotype
311 of *nlf-1* mutants. Indeed, a mutation in *egl-10*, encoding the RGS that negatively regulates G_o [92], strongly
312 enhances the *nlf-1* fainter phenotype (Fig 6D). As controls, mutations in genes involved in dense-core
313 vesicle biogenesis (*eipr-1* and *cccp-1),* that cause locomotion defects comparable to *grk-2 or egl-10* [63,80],
314 did not enhance the *nlf-1* fainter phenotype, indicating that the interactions of *grk-2* and *egl-10* with *nlf-1*
315 are specific.

316 *grk-2* acts in head acetylcholine neurons to mediate locomotion. We recently used the same *Punc-17H*
317 promoter construct to show that *nlf-1* also acts in head acetylcholine neurons and not in ventral cord
318 motor neurons to regulate locomotion [12]. Therefore, we predicted that expression of an activated G_o
319 mutant under a head acetylcholine neuron promoter would enhance the fainter phenotype of *nlf-1*
320 mutants. Indeed, we found that expression of the activated G_o mutant GOA-1[Q205L] in head
321 acetylcholine neurons makes the animals slow (Fig 6E) and significantly enhances the fainter phenotype of
322 *nlf-1* mutants (Fig 6F). These results support the model that GRK-2 negatively regulates G_o, and that G_o
323 negatively regulates NCA-1 and NCA-2 channel activity.

324

325 **Dopamine acts through DOP-3 to negatively modulate NCA-1 and NCA-2 channel activity**

326 Our results are consistent with the model that GRK-2 acts in locomotion by negatively regulating DOP-3
327 and that GRK-2 is a positive modulator of NCA-1 and NCA-2 activity. These data predict that DOP-3 would
328 be a negative modulator of NCA-1 and NCA-2 channel activity. Consistent with this model, mutations in

329 *cat-2* and *dop-3* almost fully suppress the *nlf-1* fainter phenotype during forward movement (Fig 7A and
330 7B). Additionally, *dop-3* mutants partially suppress the strong *grk-2; nlf-1* fainter phenotype, consistent
331 with the model that DOP-3 is a substrate for GRK-2 (Fig 7C). These results suggest that dopamine, through
332 DOP-3, negatively modulates NCA-1 and NCA-2 channel activity.

333 To more directly test whether *grk-2* and *dop-3* modulate the NCA channel per se, we created double
334 mutants between *grk-2* and the pore-forming subunit gene *nca-1. nca-1* mutants have a low penetrance,
335 very weak backward-fainting phenotype that is strongly enhanced in a *grk-2* mutant background (Fig S3C
336 and S6F). *arr-1* mutants, on the other hand, do not enhance the *nca-1* phenotype, further supporting the
337 conclusion that arrestin does not play a role in this pathway (Fig S3C). As expected, *dop-3* suppresses the
338 enhanced fainting phenotype of the *grk-2; nca-1* double mutant (Fig S6F).

339 Our data suggest that GRK-2 and DOP-3 play modulatory and not essential roles in the regulation of
340 NCA-1 (and possibly NCA-2) channel activity. By contrast, UNC-80 is necessary for the stability and function
341 of NCA-1 and NCA-2, so *unc-80* mutants are strong fainters [36,39]. As expected for a modulatory role in
342 regulating NCA-1 and NCA-2 activity, mutations in *dop-3* and *cat-2* do not suppress the strong fainter
343 phenotype of *unc-80* mutants (Fig S8A and S8B).

344 We showed above that *grk-2* mutants are hypersensitive to the paralytic effects of dopamine. We also
345 found that low concentrations of dopamine do not paralyze *grk-2* mutants but instead cause them to faint,
346 and that this effect depends on *dop-3* (Fig 7D). This is consistent with the model that dopamine acts
347 through DOP-3 to negatively modulate NCA-1 and NCA-2.

348

349 **GRK-2 and DOP-3 act in command interneurons to control *grk-2* dependent locomotion**

350 In *C. elegans*, the NCA channels act in premotor interneurons [12,43,91]. To determine whether *grk-2*
351 acts in a cell autonomous way to regulate NCA, we identified the head acetylcholine neurons where GRK-2
352 is expressed. We coexpressed GRK-2 fused to tagRFP driven by the *grk-2* promoter (*grk-2*::RFP) and

353 nuclear YFP driven by the choline transporter *cho-1* promoter (*Pcho-1*^{fosmid}::SL2::YFP::H2B), which is
354 expressed in all acetylcholine neurons [93]. We found that *grk-2* is expressed in the following head
355 acetylcholine neurons: the AVA, AVB, AVD, and AVE premotor interneurons; SMD and RMD head motor
356 neurons; and in the AIN, AIY, SIA, SIB, and SAA interneurons (Fig 8A).
357 To further determine where GRK-2 acts to control locomotion, we expressed the *grk-2* cDNA under
358 additional neuron-specific promoters in *grk-2* mutants. We used a *cho-1* promoter fragment for expression
359 in the SMD and RMD head motor neurons [94], the *ceh-24* promoter for expression in the SIA and SIB
360 interneurons, and a *ttx-3* promoter fragment for AIY-specific expression [95]. For expression in premotor
361 command interneurons we used a combination of the *nmr-1* promoter for AVA, AVD and AVE (also PVC
362 and RIM) expression together with the *sra-11* promoter for AVB (also AIY and AIA) expression, as
363 previously described [91]. We found that *grk-2* expression in command interneurons fully rescued the slow
364 locomotion of *grk-2* mutants, but expression in the other neuron types failed to rescue (Fig 8B-8E).
365 However, expression of *grk-2* in only *sra-11* or only *nmr-1* expressing neurons did not rescue the slow
366 locomotion defect (Fig S9). Additionally, *grk-2* expression in the command interneurons was sufficient to
367 rescue the enhanced fainting phenotype of *grk-2; nlf-1* mutants (Fig 8F). Similarly, *dop-3* expression in the
368 command interneurons was sufficient to reverse the *dop-3* suppression of the slow locomotion of *grk-2*
369 mutants (Fig 8G). Given that the fainting phenotypes of *nlf-1* mutants and *nca* mutants were also rescued
370 by expression in command interneurons [43,91], our results suggest that GRK-2, DOP-3, and the NCA
371 channels act in the same neurons. However, we did not see rescue of the *grk-2* locomotion phenotype
372 using the *glr-1* promoter (Fig 3A), which in principle is also expressed in the command interneurons, and
373 similarly we did not observe statistically significant rescue of the *nlf-1* fainting phenotype using the same
374 *glr-1* promoter [12]. The different results seen between the *glr-1* and the *nmr-1* + *sra-11* promoters may
375 be due to different levels of expression or because of expression in some different neuron types.
376

377 **Discussion**

378 In this study we identified a pathway that modulates the activity of the NCA-1 and NCA-2 channels
379 through dopamine and G_q signaling (Fig 9). We found that dopamine acts through the D2-like receptor
380 DOP-3 to negatively modulate NCA-1 and NCA-2. Furthermore, we identified the GPCR kinase GRK-2 as a
381 positive (indirect) regulator of G_q and negative regulator of NCA-1 and NCA-2. Our results suggest that
382 GRK-2 mediates its regulatory effects by inhibiting DOP-3.

383 In *C. elegans*, GRK-2 was previously found to act in sensory neurons to regulate chemosensation [52].
384 Here we found that GRK-2 acts in command interneurons to regulate locomotion and G_q signaling. Using a
385 structure-function approach, we found that GPCR phosphorylation, Gβγ-binding, and membrane-binding
386 are required for GRK-2 function in locomotion, but binding to G_q is not required. Similar results were
387 reported for the function of GRK-2 in chemosensation [48], suggesting that in both cases GRK-2 acts as a
388 GPCR kinase and that membrane localization is critical for its function. Additionally, GRK-2 seems to act
389 independently of arrestin to regulate both locomotion and chemosensation [52]. Because *cat-2* and *dop-3*
390 mutants are hypersensitive to the aversive odorant octanol [96–98] and *grk-2* mutants are insensitive to
391 octanol [52], GRK-2 might act as a GPCR kinase for DOP-3 in chemosensory neurons as well.

392 GRK-induced phosphorylation of GPCRs induces endocytosis, which leads to their sorting to either
393 lysosomes for degradation or to recycling endosomes. GRK-dependent recruitment of arrestins to the
394 phosphorylated receptor is typically required for endocytosis, but GRK2 was also reported to utilize
395 arrestin-independent mechanisms to mediate receptor internalization [66]. GRK2 associates with a large
396 number of proteins with known roles in receptor internalization and signaling. For example, the C-
397 terminus of GRK2 directly binds clathrin and this interaction has been proposed to be involved in arrestin-
398 independent internalization [99]. Our data suggest an arrestin-independent role for *C. elegans* GRK-2 in
399 GPCR regulation, supporting the idea that the role of GRK-2 extends beyond just the recruitment of
400 arrestin.

401 The D2-type dopamine receptors, like DOP-3, are GPCRs that couple to members of the inhibitory $G_{i/o}$
402 family. Mammalian GRK2 and GRK3 (the orthologs of GRK-2) have been connected to the desensitization,
403 internalization, and recycling of D2-type dopamine receptors [55–59,100]. Interestingly, some of the
404 effects of GRK2 on D2 receptor function may be independent of receptor phosphorylation [57,58,100],
405 though one caveat of these studies is that they involve GRK2 overexpression in heterologous cells. Our
406 structure-function approach indicates that GPCR phosphorylation is important for GRK-2 function in
407 locomotion and G_q signaling in *C. elegans*, although we cannot exclude the possibility that phosphorylation
408 of additional substrates may also be required. *In vivo* studies of the role of mammalian GRKs in the
409 regulation of dopamine receptors have focused on the analysis of behaviors that are induced by
410 psychostimulatory drugs such as cocaine that elevate the extracellular concentration of dopamine [59].
411 Mice with a cell-specific knockout of GRK2 in D2 receptor-expressing neurons have altered spontaneous
412 locomotion and sensitivity to cocaine [101], though the cellular mechanisms underlying these behavioral
413 effects are not known. Our findings provide evidence of a direct association between GRK-2 and D2-type
414 receptor signaling that regulates locomotion in an *in vivo* system.

415 In *C. elegans,* the G_q and G_o pathways act in opposite ways to regulate locomotion by controlling
416 synaptic vesicle release [82]. G_q acts as a positive regulator of acetylcholine release while G_o negatively
417 regulates G_q signaling, through activation of the G_q RGS EAT-16 and the diacylglycerol kinase DGK-1. DGK-1
418 phosphorylates the second messenger DAG and thus inhibits its action. Using genetic epistasis, we
419 demonstrated that GRK-2 acts upstream of GOA-1/G_o and EAT-16 to positively regulate locomotion and
420 body posture. Given this result, our cell-specific rescue data, and our data indicating that GRK-2 acts as a
421 GPCR kinase for a locomotion-related GPCR, we propose that GRK-2 acts as a kinase for the G_o-coupled
422 GPCR DOP-3 in premotor interneurons. In this model, GRK-2 driven phosphorylation of DOP-3 reduces G_o
423 signaling and thereby activates G_q signaling (Fig 9). Inhibition of G_o by GRK-2 could promote G_q-Rho

424 signaling by two mechanisms: (1) by inhibiting the G_q RGS EAT-16 and thus activating G_q itself, and (2) by
425 inhibiting DGK-1 which acts in parallel to G_q-Rho to regulate DAG levels (Fig 9).

426 Interestingly, a *grk-2* mutant is suppressed by mutations in *goa-1* and *eat-16*, but not by *dgk-1*. This
427 finding supports other literature that suggests that *goa-1* and *eat-16* have similar interactions with G_q
428 signaling, but that *dgk-1* is distinct [87,102]. GOA-1 and EAT-16 act upstream of G_q to inhibit G_q signaling.
429 DGK-1, on the other hand, acts downstream of G_q to reduce the pool of the G_q-generated second
430 messenger DAG. Adding to the complexity, DAG levels may be controlled by both the PLCβ and Rho
431 branches of the G_q pathway (Fig 9). Previously, it has been shown that mutations in *dgk-1* partially
432 suppress the strong locomotion defect of *egl-30*/G_q loss-of-function mutations [102]. Surprisingly, we
433 found that a *grk-2* mutation fully suppresses a *dgk-1* mutant. This suggests that the effect of GRK-2 on
434 locomotion is more complex and may be partially independent of G_q signaling and of G_q-generated DAG.
435 This agrees with our data showing that GRK-2 has additional neuronal functions that do not depend on
436 DOP-3.

437 G_q signaling regulates several genetically separable aspects of locomotion behavior including
438 locomotion rate and waveform. The G_q-PLCβ signaling pathway has been reported to act in ventral cord
439 motor neurons to regulate acetylcholine release and locomotion rate [103], whereas the G_q-Rho pathway
440 has been reported to act in at least two different classes of neurons including head acetylcholine neurons
441 to regulate locomotion rate, waveform, and fainting behavior [12]. Our data here further suggest that
442 DOP-3, GRK-2, and the G_q-Rho pathway all act together in the premotor command interneurons to
443 regulate activity of the NCA channels. The command interneurons have been previously shown to regulate
444 several aspects of locomotion behavior including the propensity to go forward or reverse [104,105] and
445 the tendency of the worm to sustain persistent locomotion [43]. Our data here suggest that the command
446 interneurons also regulate the locomotion rate and the posture of the animals. As we reported previously,
447 mutations in the Rho-NCA pathway suppress both the locomotion rate and loopy posture of activated G_q

448 mutants whereas mutations in the PLCβ pathway suppress mainly the locomotion rate [12]. Thus, G_q acts
449 through both the PLCβ pathway and the Rho-NCA pathway to regulate locomotion rate, probably by acting
450 in different neurons. By contrast, G_q acts primarily through the Rho-NCA pathway to regulate the posture
451 of the worms. This agrees with our data showing that *grk-2* mutations, which affect signaling through the
452 Rho-NCA pathway, strongly suppress the loopy posture of activated G_q.

453 The identification of GRK-2 as a putative DOP-3 kinase and positive modulator of G_q-Rho signaling
454 connects dopamine signaling to modulation of the NCA channels (Fig 9). NCA channels have been shown in
455 recent years to be important for neuronal excitability and a number of rhythmic behaviors [16,34–42]. In
456 humans, mutations affecting the NCA channel NALCN cause neurological diseases [20–33]. However,
457 despite the relevance of this channel to neuronal function it is unclear how it is gated and activated. Two
458 studies have shown that NALCN-dependent currents can be activated by G protein-coupled receptors in a
459 G-protein independent way [44,45] whereas another study showed that NALCN can be activated by low
460 extracellular calcium via a G protein-dependent pathway [46], but the specific mechanisms remain
461 unknown. Our results suggest that dopamine acts through the DOP-3 G-protein coupled receptor and
462 downstream G protein signaling pathways to modulate activity of the NCA channels in a physiologically
463 relevant setting. This is the first study connecting dopamine to the activation of these important channels.
464

465 ## Methods

466 **Strains**

467 Strains were maintained at room temperature or 20° on the OP50 strain of *E. coli* [106].
468 The Supplementary Information contains full genotypes of all the strains we used (S1 Table; List of strains).

469

470 **Isolation and identification of the *grk-2(yak18)* mutation**

471 The *grk-2(yak18)* mutant was isolated in an ENU screen as a suppressor of the hyperactive locomotion
472 and loopy posture of the activated G_q mutant *egl-30(tg26)* [63]. We mapped the *yak18* mutation to the left
473 arm of Chromosome III (between -27 and -21.8 m.u.) using a PCR mapping strategy that takes advantage of
474 PCR length polymorphisms due to indels in the Hawaiian strain CB4856 (Jihong Bai, personal
475 communication). Using whole-genome sequencing (see below), we found that *yak18* is a G to A transition
476 mutation in the W02B3.2 *(grk-2*) ORF that creates a G379E missense mutation in the kinase domain of
477 GRK-2. We confirmed the gene identification by performing a complementation test between *grk-2(yak18)*
478 and the *grk-2(gk268)* deletion mutant, finding that they fail to complement for the slow locomotion
479 phenotype.

480

481 **Whole-Genome Sequencing**

482 Genomic DNA from *grk-2(yak18)* animals was isolated and purified according to the Worm Genomic
483 DNA prep protocol from the Hobert lab website (http://hobertlab.org/wp-
484 content/uploads/2013/02/Worm_Genomic_DNA_Prep.pdf). The sample was sequenced using Ion Torrent
485 sequencing (DNA Sequencing Core Facility, University of Utah). The sequencing data were uploaded to the
486 Galaxy web platform and were analyzed as described [107].

487

488 **Constructs and transgenes**

489 The Supplemental Information contains a complete list of constructs used (S2 Table; List of plasmids).
490 All constructs made in this study were constructed using the multisite Gateway system (Invitrogen).
491 Specifically, a promoter region, a gene region (cDNA), and an N- or C-terminal 3'UTR or fluorescent tag
492 (GFP or tagRFP) fused to a 3'UTR were cloned into the destination vector pCFJ150. For the cell-specific
493 rescuing experiments, an operon GFP was included in the expression constructs downstream of the 3'UTR
494 [108]. This resulted in expression of untagged *grk-2, dop-3,* or *goa-1*, but allowed for confirmation of
495 proper promoter expression by monitoring GFP expression. The *cho-1* fosmid reporter construct *otIs534*
496 carries an SL2-spliced nuclear localized YFP::H2B immediately after the stop codon of the *cho-1* gene [93].
497 Extrachromosomal arrays were made by standard injection and transformation methods [109]. In all
498 cases we injected 5-10 ng/ul of the expression vector and isolated multiple independent lines. At least two
499 lines were tested that behaved similarly.
500
501 **Expression of *grk-2***
502 We made a construct driving expression of the *grk-2* cDNA fused to tagRFP under the *grk-2* promoter
503 and generated worms with extrachromosomal arrays. For the *grk-2* promoter region, we PCR amplified
504 2892 bp upstream of the start codon using genomic DNA as a template and the following set of primers:
505 forward primer 5'cacgacagtttccatagtgattgg3' and reverse primer 5'tttttgttctgcaaaatcgaattg3'. *grk-2* was
506 expressed in neurons in the head, ventral cord, and tail, consistent with the published expression pattern
507 [52]. Neurons were identified by the stereotypical positions of cells expressing the acetylcholine neuron
508 reporter *cho-1*^{fosmid}::SL2::YFP::H2B [93,110] that colocalized with *grk-2*::tagRFP.
509
510 **Locomotion and egg-laying assays**
511 For most experiments, we measured locomotion rate using the body bend assay. Specifically, first-day
512 adults were picked to a three-day-old lawn of OP50 and stimulated by poking the tail of the animal with a

513 worm pick. Body bends were then immediately counted for one minute. A body bend was defined as the
514 movement of the worm from maximum to minimum amplitude of the sine wave [102]. Specifically for the
515 experiment described in Fig 5D we used a radial locomotion assay. Animals were placed in the center of 10
516 cm plates with thin one to two-day-old lawns of OP50 and left for one hour. The position of each worm
517 was marked and the radial distance from the center of the plate was measured (cm travelled/h).
518 Egg-laying assays were performed as described [80]. L4 larvae were placed on plates with OP50 at 25°C
519 overnight. The next day, five animals were moved to a fresh plate and allowed to lay eggs at 25°C for two
520 hours. The number of eggs present on the plate was counted.
521
522 **Waveform quantification**
523 First-day adult animals were placed on an OP50 plate and allowed to move forward until when they
524 had completed five to ten tracks. Each animal's tracks were imaged at 40X magnification using a Nikon
525 SMZ18 microscope with the DS-L3 camera control system. Period and 2X amplitude were measured using
526 the line tool in Image J. For each worm, five period/ amplitude ratios were averaged and five worms were
527 used per experiment.
528
529 **Fainting assays**
530 The fainting phenotype is characterized by frequent arrest of locomotion, accompanied by a
531 straightening of the anterior part of the body. We scored fainting as a sudden halt in movement
532 accompanied by a straightened posture.
533 First-day adults were transferred to plates with two to three-day-old lawns of OP50 and left
534 undisturbed for one minute. Animals were then poked either on the head (for backward movement) or on
535 the tail (for forward movement), and we counted the number of body bends before the animal faints. If
536 the animal made ten body bends, the assay was stopped and we recorded ten as the number. Thus,

537 animals that never faint (for example, wild-type) are scored as 10 in these experiments. Specifically for the
538 experiment described in Fig 7D the number reported was the percentage of animals that fainted before
539 making 10 body bends.
540
541 **Swimming assays**
542 Single, first-day adults were transferred to a 25 ul drop of M9 buffer at the center of an empty NGM
543 plate and video recorded for 30 sec. The swimming behavior was analyzed as described [38,64].
544
545 **Body length measurements**
546 First-day adults were mounted on 2% agarose pads and anesthetized in M9 buffer containing 50 mM
547 sodium azide for ten minutes. The image of each animal was obtained using a Nikon 80i wide-field
548 compound microscope. Body size was measured using ImageJ software.
549
550 **Dopamine resistance assays**
551 We used a method similar to the one described [61]. Specifically, first-day adults were transferred to
552 plates containing dopamine (5 mM, 10 mM, 15 mM, 20 mM, 40 mM) and incubated for 20 min at room
553 temperature. Animals were then poked using a worm-pick and the number of body bends was counted,
554 stopping the assay at 10 body bends. We report the percent of animals that moved 10 body bends without
555 stopping (Percent of animals moving). A body bend was defined as the movement of the worm from
556 maximum to minimum amplitude of the sine wave. Dopamine plates were prepared fresh just before use,
557 as described [61].
558

559 **Immunoblotting**

560 For the Western analysis shown in Figure 2G, worm lysates were prepared as follows. Ten transgenic
561 animals from each strain were transferred to a 6 cm OP50 plate and grown until most of their progeny had
562 reached adult stage. Animals from five such plates were washed off with M9, collected in a 15 ml Falcon
563 tube, and spun down at 2000 rpm for 3 min. Animals were washed twice with M9. The pelleted worms
564 were then resuspended in 2X SDS loading dye and lysed by incubation at 95°C for 20 min. For the Western
565 analysis shown in Figure S7B, worm lysates were prepared as follows. Two hundred transgenic worms
566 were individually picked and transferred in a microfuge tube in 10 ul M9. An equal volume of 2X SDS
567 loading dye was added to the tube and the animals were lysed by incubation at 95°C for 20 min.

568 Samples were resolved on 10% SDS-polyacrylamide gels and blotted onto PVDF membranes. To detect
569 the desired proteins, we added the following primary antibodies: monoclonal anti-GRK2/3, clone C5/1.1
570 (1:1000, EMD Millipore #05-465), monoclonal anti-beta-tubulin antibody (1:1000, ThermoFisher, BT7R,
571 #MA5-16308), rabbit polyclonal anti-GFP (1:1000, Santa Cruz #sc-8334), and monoclonal anti-mCherry
572 (1:50, a gift from Jihong Bai and the Fred Hutchinson Cancer Research Center antibody development
573 shared resource center). The secondary antibodies were an Alexa Fluor 680-conjugated goat anti-mouse
574 antibody (1:20,000, Jackson Laboratory #115-625-144) and an Alexa Fluor 680-conjugated goat anti-rabbit
575 antibody (1:20,000, Jackson Laboratory #115-625-166). A LI-COR processor was used to develop images.

576

577 **Imaging**

578 For fluorescence imaging, first-day adult animals were mounted on 2% agarose pads and anesthetized
579 with 50 mM sodium azide for ten minutes before placing the cover slip. The images shown in Figures 3D
580 and S7C were obtained using an Olympus FLUOVIEW FV1200 confocal microscope. The images shown in
581 Figure 8A were acquired using a Zeiss confocal microscope (LSM880) with Z-stack analysis and
582 reconstruction performed using the ZEN software tool.

583 For pictures of worms, first-day adult animals were placed on an assay plate and photographed at 50
584 or 60X using a Nikon SMZ18 dissecting microscope with a DS-L3 camera control system. The images were
585 processed using ImageJ.
586
587 **Statistics**
588 P values were determined using GraphPad Prism 5.0d (GraphPad Software). Normally distributed data
589 sets requiring multiple comparisons were analyzed by a one-way ANOVA followed by a Bonferroni or
590 Dunnett test. Normally distributed pairwise data comparisons were analyzed by two-tailed unpaired t
591 tests. Non-normally distributed data sets with multiple comparisons were analyzed by a Kruskal-Wallis
592 nonparametric ANOVA followed by Dunn's test to examine selected comparisons. Non-normally
593 distributed pairwise data comparisons were analyzed by a Mann-Whitney test. For the experiments shown
594 in Figures S3C and S6F a chi-square test for multiple comparisons was used.
595

596 ## Acknowledgments

597 Special thanks to Denise Ferkey and Jordan Wood for generously providing the *grk-2* mutant
598 constructs, Jihong Bai for discussions and sharing unpublished methods and equipment, Yongming Dong
599 for help with the swimming assay, Ithai Rabinowitch for the *sra-11* promoter plasmid, Jill Hoyt for making
600 the *grk-2; nlf-1* double mutant, Jill Hoyt and Jordan Hoyt for help with the analysis of the whole-genome
601 sequencing data, Jérôme Cattin-Ortolá for help with confocal microscopy, Dana Miller for sharing
602 equipment, Oliver Hobert for providing materials and methodology, and Brian Kraemer and Rebecca Kow
603 for insightful ideas. Some strains were provided by the CGC, which is funded by the NIH Office of Research
604 Infrastructure Programs (P40 OD010440).
605

606 ## Author Contributions

607 IT and MA conceived and designed the experiments. IT and KC performed the experiments. LP identified
608 the head acetylcholine neurons where *grk-2* is expressed. IT and MA wrote the paper.

609 ## References

610 1. Wilkie TM, Gilbert DJ, Olsen AS, Chen XN, Amatruda TT, Korenberg JR, et al. Evolution of the
611 mammalian G protein alpha subunit multigene family. Nat Genet. 1992;1: 85–91.
612 doi:10.1038/ng0592-85

613 2. Coulon P, Kanyshkova T, Broicher T, Munsch T, Wettschureck N, Seidenbecher T, et al. Activity Modes
614 in Thalamocortical Relay Neurons are Modulated by G(q)/G(11) Family G-proteins - Serotonergic and
615 Glutamatergic Signaling. Front Cell Neurosci. 2010;4: 132. doi:10.3389/fncel.2010.00132

616 3. Gamper N, Reznikov V, Yamada Y, Yang J, Shapiro MS. Phosphatidylinositol 4,5-bisphosphate signals
617 underlie receptor-specific Gq/11-mediated modulation of N-type Ca2+ channels. J Neurosci. 2004;24:
618 10980–10992. doi:10.1523/JNEUROSCI.3869-04.2004

619 4. Krause M, Offermanns S, Stocker M, Pedarzani P. Functional specificity of G alpha q and G alpha 11 in
620 the cholinergic and glutamatergic modulation of potassium currents and excitability in hippocampal
621 neurons. J Neurosci. 2002;22: 666–673.

622 5. Lutz S, Freichel-Blomquist A, Yang Y, Rümenapp U, Jakobs KH, Schmidt M, et al. The guanine
623 nucleotide exchange factor p63RhoGEF, a specific link between Gq/11-coupled receptor signaling and
624 RhoA. J Biol Chem. 2005;280: 11134–11139. doi:10.1074/jbc.M411322200

625 6. Lutz S, Shankaranarayanan A, Coco C, Ridilla M, Nance MR, Vettel C, et al. Structure of Galphaq-
626 p63RhoGEF-RhoA complex reveals a pathway for the activation of RhoA by GPCRs. Science. 2007;318:
627 1923–1927. doi:10.1126/science.1147554

628 7. Rojas RJ, Yohe ME, Gershburg S, Kawano T, Kozasa T, Sondek J. Galphaq directly activates p63RhoGEF
629 and Trio via a conserved extension of the Dbl homology-associated pleckstrin homology domain. J
630 Biol Chem. 2007;282: 29201–29210. doi:10.1074/jbc.M703458200

631 8. Williams SL, Lutz S, Charlie NK, Vettel C, Ailion M, Coco C, et al. Trio's Rho-specific GEF domain is the
632 missing Galpha q effector in C. elegans. Genes Dev. 2007;21: 2731–2746. doi:10.1101/gad.1592007

633 9. Chan JP, Hu Z, Sieburth D. Recruitment of sphingosine kinase to presynaptic terminals by a conserved
634 muscarinic signaling pathway promotes neurotransmitter release. Genes Dev. 2012;26: 1070–1085.
635 doi:10.1101/gad.188003.112

636 10. Hiley E, McMullan R, Nurrish SJ. The Galpha12-RGS RhoGEF-RhoA signalling pathway regulates
637 neurotransmitter release in C. elegans. EMBO J. 2006;25: 5884–5895. doi:10.1038/sj.emboj.7601458

638 11. McMullan R, Hiley E, Morrison P, Nurrish SJ. Rho is a presynaptic activator of neurotransmitter
639 release at pre-existing synapses in C. elegans. Genes Dev. 2006;20: 65–76. doi:10.1101/gad.359706

640 12. Topalidou I, Chen P-A, Cooper K, Watanabe S, Jorgensen EM, Ailion M. The NCA-1 and NCA-2 ion
641 channels function downstream of Gq and Rho to regulate locomotion in Caenorhabditis elegans.
642 Genetics. 2017;206: 265–282. doi:10.1534/genetics.116.198820

643 13. Ren D. Sodium leak channels in neuronal excitability and rhythmic behaviors. Neuron. 2011;72: 899–
644 911. doi:10.1016/j.neuron.2011.12.007

645 14. Liebeskind BJ, Hillis DM, Zakon HH. Phylogeny unites animal sodium leak channels with fungal calcium
646 channels in an ancient, voltage-insensitive clade. Mol Biol Evol. 2012;29: 3613–3616.
647 doi:10.1093/molbev/mss182

648 15. Lee JH, Cribbs LL, Perez-Reyes E. Cloning of a novel four repeat protein related to voltage-gated
649 sodium and calcium channels. FEBS Lett. 1999;445: 231–236.

650 16. Lu B, Su Y, Das S, Liu J, Xia J, Ren D. The neuronal channel NALCN contributes resting sodium
651 permeability and is required for normal respiratory rhythm. Cell. 2007;129: 371–383.
652 doi:10.1016/j.cell.2007.02.041

653 17. Boone AN, Senatore A, Chemin J, Monteil A, Spafford JD. Gd3+ and calcium sensitive, sodium leak
654 currents are features of weak membrane-glass seals in patch clamp recordings. PloS One. 2014;9:
655 e98808. doi:10.1371/journal.pone.0098808

656 18. Senatore A, Spafford JD. A uniquely adaptable pore is consistent with NALCN being an ion sensor.
657 Channels. 2013;7: 60–68. doi:10.4161/chan.23981

658 19. Senatore A, Monteil A, van Minnen J, Smit AB, Spafford JD. NALCN ion channels have alternative
659 selectivity filters resembling calcium channels or sodium channels. PloS One. 2013;8: e55088.
660 doi:10.1371/journal.pone.0055088

661 20. Al-Sayed MD, Al-Zaidan H, Albakheet A, Hakami H, Kenana R, Al-Yafee Y, et al. Mutations in NALCN
662 cause an autosomal-recessive syndrome with severe hypotonia, speech impairment, and cognitive
663 delay. Am J Hum Genet. 2013;93: 721–726. doi:10.1016/j.ajhg.2013.08.001

664 21. Chong JX, McMillin MJ, Shively KM, Beck AE, Marvin CT, Armenteros JR, et al. De novo mutations in
665 NALCN cause a syndrome characterized by congenital contractures of the limbs and face, hypotonia,
666 and developmental delay. Am J Hum Genet. 2015;96: 462–473. doi:10.1016/j.ajhg.2015.01.003

667 22. Fukai R, Saitsu H, Okamoto N, Sakai Y, Fattal-Valevski A, Masaaki S, et al. De novo missense mutations
668 in NALCN cause developmental and intellectual impairment with hypotonia. J Hum Genet. 2016;61:
669 451–455. doi:10.1038/jhg.2015.163

670 23. Aoyagi K, Rossignol E, Hamdan FF, Mulcahy B, Xie L, Nagamatsu S, et al. A Gain-of-Function Mutation
671 in NALCN in a Child with Intellectual Disability, Ataxia, and Arthrogryposis. Hum Mutat. 2015;36: 753–
672 757. doi:10.1002/humu.22797

673 24. Bend EG, Si Y, Stevenson DA, Bayrak-Toydemir P, Newcomb TM, Jorgensen EM, et al. NALCN
674 channelopathies: Distinguishing gain-of-function and loss-of-function mutations. Neurology. 2016;87:
675 1131–1139. doi:10.1212/WNL.0000000000003095

676 25. Gal M, Magen D, Zahran Y, Ravid S, Eran A, Khayat M, et al. A novel homozygous splice site mutation
677 in NALCN identified in siblings with cachexia, strabismus, severe intellectual disability, epilepsy and
678 abnormal respiratory rhythm. Eur J Med Genet. 2016;59: 204–209. doi:10.1016/j.ejmg.2016.02.007

679 26. Karakaya M, Heller R, Kunde V, Zimmer K-P, Chao C-M, Nürnberg P, et al. Novel Mutations in the
680 Nonselective Sodium Leak Channel (NALCN) Lead to Distal Arthrogryposis with Increased Muscle
681 Tone. Neuropediatrics. 2016;47: 273–277. doi:10.1055/s-0036-1584084

682 27. Köroğlu Ç, Seven M, Tolun A. Recessive truncating NALCN mutation in infantile neuroaxonal
683 dystrophy with facial dysmorphism. J Med Genet. 2013;50: 515–520. doi:10.1136/jmedgenet-2013-
684 101634

685 28. Perez Y, Kadir R, Volodarsky M, Noyman I, Flusser H, Shorer Z, et al. UNC80 mutation causes a
686 syndrome of hypotonia, severe intellectual disability, dyskinesia and dysmorphism, similar to that
687 caused by mutations in its interacting cation channel NALCN. J Med Genet. 2016;53: 397–402.
688 doi:10.1136/jmedgenet-2015-103352

689 29. Valkanas E, Schaffer K, Dunham C, Maduro V, du Souich C, Rupps R, et al. Phenotypic evolution of
690 UNC80 loss of function. Am J Med Genet A. 2016;170: 3106–3114. doi:10.1002/ajmg.a.37929

691 30. Shamseldin HE, Faqeih E, Alasmari A, Zaki MS, Gleeson JG, Alkuraya FS. Mutations in UNC80, Encoding
692 Part of the UNC79-UNC80-NALCN Channel Complex, Cause Autosomal-Recessive Severe Infantile
693 Encephalopathy. Am J Hum Genet. 2016;98: 210–215. doi:10.1016/j.ajhg.2015.11.013

694 31. Stray-Pedersen A, Cobben J-M, Prescott TE, Lee S, Cang C, Aranda K, et al. Biallelic Mutations in
695 UNC80 Cause Persistent Hypotonia, Encephalopathy, Growth Retardation, and Severe Intellectual
696 Disability. Am J Hum Genet. 2016;98: 202–209. doi:10.1016/j.ajhg.2015.11.004

697 32. Wang Y, Koh K, Ichinose Y, Yasumura M, Ohtsuka T, Takiyama Y. A de novo mutation in the NALCN
698 gene in an adult patient with cerebellar ataxia associated with intellectual disability and
699 arthrogryposis. Clin Genet. 2016;90: 556–557. doi:10.1111/cge.12851

700 33. Lozic B, Johansson S, Lovric Kojundzic S, Markic J, Knappskog PM, Hahn AF, et al. Novel NALCN
701 variant: altered respiratory and circadian rhythm, anesthetic sensitivity. Ann Clin Transl Neurol.
702 2016;3: 876–883. doi:10.1002/acn3.362

703 34. Funato H, Miyoshi C, Fujiyama T, Kanda T, Sato M, Wang Z, et al. Forward-genetics analysis of sleep in
704 randomly mutagenized mice. Nature. 2016;539: 378–383. doi:10.1038/nature20142

705 35. Humphrey JA, Hamming KS, Thacker CM, Scott RL, Sedensky MM, Snutch TP, et al. A putative cation
706 channel and its novel regulator: cross-species conservation of effects on general anesthesia. Curr Biol.
707 2007;17: 624–629. doi:10.1016/j.cub.2007.02.037

708 36. Jospin M, Watanabe S, Joshi D, Young S, Hamming K, Thacker C, et al. UNC-80 and the NCA ion
709 channels contribute to endocytosis defects in synaptojanin mutants. Curr Biol. 2007;17: 1595–1600.
710 doi:10.1016/j.cub.2007.08.036

711 37. Nash HA, Scott RL, Lear BC, Allada R. An unusual cation channel mediates photic control of
712 locomotion in Drosophila. Curr Biol. 2002;12: 2152–2158.

713 38. Pierce-Shimomura JT, Chen BL, Mun JJ, Ho R, Sarkis R, McIntire SL. Genetic analysis of crawling and
714 swimming locomotory patterns in C. elegans. Proc Natl Acad Sci U S A. 2008;105: 20982–20987.
715 doi:10.1073/pnas.0810359105

716 39. Yeh E, Ng S, Zhang M, Bouhours M, Wang Y, Wang M, et al. A putative cation channel, NCA-1, and a
717 novel protein, UNC-80, transmit neuronal activity in C. elegans. PLoS Biol. 2008;6: e55.
718 doi:10.1371/journal.pbio.0060055

719 40. Lear BC, Darrah EJ, Aldrich BT, Gebre S, Scott RL, Nash HA, et al. UNC79 and UNC80, Putative Auxiliary
720 Subunits of the NARROW ABDOMEN Ion Channel, Are Indispensable for Robust Circadian Locomotor
721 Rhythms in Drosophila. PloS One. 2013;8: e78147. doi:10.1371/journal.pone.0078147

722 41. Lear BC, Lin J-M, Keath JR, McGill JJ, Raman IM, Allada R. The ion channel narrow abdomen is critical
723 for neural output of the Drosophila circadian pacemaker. Neuron. 2005;48: 965–976.
724 doi:10.1016/j.neuron.2005.10.030

725 42. Yeh S-Y, Huang W-H, Wang W, Ward CS, Chao ES, Wu Z, et al. Respiratory Network Stability and
726 Modulatory Response to Substance P Require Nalcn. Neuron. 2017;94: 294–303.
727 doi:10.1016/j.neuron.2017.03.024

728 43. Gao S, Xie L, Kawano T, Po MD, Pirri JK, Guan S, et al. The NCA sodium leak channel is required for
729 persistent motor circuit activity that sustains locomotion. Nat Commun. 2015;6: 6323.
730 doi:10.1038/ncomms7323

731 44. Lu B, Su Y, Das S, Wang H, Wang Y, Liu J, et al. Peptide neurotransmitters activate a cation channel
732 complex of NALCN and UNC-80. Nature. 2009;457: 741–744. doi:10.1038/nature07579

733 45. Swayne LA, Mezghrani A, Varrault A, Chemin J, Bertrand G, Dalle S, et al. The NALCN ion channel is
734 activated by M3 muscarinic receptors in a pancreatic beta-cell line. EMBO Rep. 2009;10: 873–880.
735 doi:10.1038/embor.2009.125

736 46. Lu B, Zhang Q, Wang H, Wang Y, Nakayama M, Ren D. Extracellular calcium controls background
737 current and neuronal excitability via an UNC79-UNC80-NALCN cation channel complex. Neuron.
738 2010;68: 488–499. doi:10.1016/j.neuron.2010.09.014

739 47. Ferguson SS. Evolving concepts in G protein-coupled receptor endocytosis: the role in receptor
740 desensitization and signaling. Pharmacol Rev. 2001;53: 1–24.

741 48. Wood JF, Wang J, Benovic JL, Ferkey DM. Structural domains required for Caenorhabditis elegans G
742 protein-coupled receptor kinase 2 (GRK-2) function in vivo. J Biol Chem. 2012;287: 12634–12644.
743 doi:10.1074/jbc.M111.336818

744 49. Benovic JL, Onorato JJ, Arriza JL, Stone WC, Lohse M, Jenkins NA, et al. Cloning, expression, and
745 chromosomal localization of beta-adrenergic receptor kinase 2. A new member of the receptor kinase
746 family. J Biol Chem. 1991;266: 14939–14946.

747 50. Schleicher S, Boekhoff I, Arriza J, Lefkowitz RJ, Breer H. A beta-adrenergic receptor kinase-like enzyme
748 is involved in olfactory signal termination. Proc Natl Acad Sci U S A. 1993;90: 1420–1424.

749 51. Jaber M, Koch WJ, Rockman H, Smith B, Bond RA, Sulik KK, et al. Essential role of beta-adrenergic
750 receptor kinase 1 in cardiac development and function. Proc Natl Acad Sci U S A. 1996;93: 12974–
751 12979.

752 52. Fukuto HS, Ferkey DM, Apicella AJ, Lans H, Sharmeen T, Chen W, et al. G protein-coupled receptor
753 kinase function is essential for chemosensation in C. elegans. Neuron. 2004;42: 581–593.

754 53. Wang J, Luo J, Aryal DK, Wetsel WC, Nass R, Benovic JL. G protein-coupled receptor kinase-2 (GRK-2)
755 regulates serotonin metabolism through the monoamine oxidase AMX-2 in Caenorhabditis elegans. J
756 Biol Chem. 2017;292: 5943–5956. doi:10.1074/jbc.M116.760850

757 54. Pierce KL, Premont RT, Lefkowitz RJ. Seven-transmembrane receptors. Nat Rev Mol Cell Biol. 2002;3:
758 639–650. doi:10.1038/nrm908

759 55. Ito K, Haga T, Lameh J, Sadée W. Sequestration of dopamine D2 receptors depends on coexpression
760 of G-protein-coupled receptor kinases 2 or 5. Eur J Biochem. 1999;260: 112–119. doi:10.1046/j.1432-
761 1327.1999.00125.x

762 56. Kim KM, Valenzano KJ, Robinson SR, Yao WD, Barak LS, Caron MG. Differential regulation of the
763 dopamine D2 and D3 receptors by G protein-coupled receptor kinases and beta-arrestins. J Biol
764 Chem. 2001;276: 37409–37414. doi:10.1074/jbc.M106728200

765 57. Cho D, Zheng M, Min C, Ma L, Kurose H, Park JH, et al. Agonist-induced endocytosis and receptor
766 phosphorylation mediate resensitization of dopamine D(2) receptors. Mol Endocrinol. 2010;24: 574–
767 586. doi:10.1210/me.2009-0369

768 58. Namkung Y, Dipace C, Javitch JA, Sibley DR. G protein-coupled receptor kinase-mediated
769 phosphorylation regulates post-endocytic trafficking of the D2 dopamine receptor. J Biol Chem.
770 2009;284: 15038–15051. doi:10.1074/jbc.M900388200

771 59. Gurevich EV, Gainetdinov RR, Gurevich VV. G protein-coupled receptor kinases as regulators of
772 dopamine receptor functions. Pharmacol Res. 2016;111: 1–16. doi:10.1016/j.phrs.2016.05.010

773 60. Sawin ER, Ranganathan R, Horvitz HR. C. elegans locomotory rate is modulated by the environment
774 through a dopaminergic pathway and by experience through a serotonergic pathway. Neuron.
775 2000;26: 619–631.

776 61. Chase DL, Pepper JS, Koelle MR. Mechanism of extrasynaptic dopamine signaling in Caenorhabditis
777 elegans. Nat Neurosci. 2004;7: 1096–1103. doi:10.1038/nn1316

778 62. Doi M, Iwasaki K. Regulation of retrograde signaling at neuromuscular junctions by the novel C2
779 domain protein AEX-1. Neuron. 2002;33: 249–259.

780 63. Ailion M, Hannemann M, Dalton S, Pappas A, Watanabe S, Hegermann J, et al. Two Rab2 interactors
781 regulate dense-core vesicle maturation. Neuron. 2014;82: 167–180.
782 doi:10.1016/j.neuron.2014.02.017

783 64. Vidal-Gadea A, Topper S, Young L, Crisp A, Kressin L, Elbel E, et al. Caenorhabditis elegans selects
784 distinct crawling and swimming gaits via dopamine and serotonin. Proc Natl Acad Sci U S A. 2011;108:
785 17504–17509. doi:10.1073/pnas.1108673108

786 65. Pitcher JA, Freedman NJ, Lefkowitz RJ. G protein-coupled receptor kinases. Annu Rev Biochem.
787 1998;67: 653–692. doi:10.1146/annurev.biochem.67.1.653

788 66. Evron T, Daigle TL, Caron MG. GRK2: multiple roles beyond G protein-coupled receptor
789 desensitization. Trends Pharmacol Sci. 2012;33: 154–164. doi:10.1016/j.tips.2011.12.003

790 67. Ribas C, Penela P, Murga C, Salcedo A, García-Hoz C, Jurado-Pueyo M, et al. The G protein-coupled
791 receptor kinase (GRK) interactome: role of GRKs in GPCR regulation and signaling. Biochim Biophys
792 Acta. 2007;1768: 913–922. doi:10.1016/j.bbamem.2006.09.019

793 68. Kong G, Penn R, Benovic JL. A beta-adrenergic receptor kinase dominant negative mutant attenuates
794 desensitization of the beta 2-adrenergic receptor. J Biol Chem. 1994;269: 13084–13087.

795 69. Pao CS, Barker BL, Benovic JL. Role of the amino terminus of G protein-coupled receptor kinase 2 in
796 receptor phosphorylation. Biochemistry (Mosc). 2009;48: 7325–7333. doi:10.1021/bi900408g

797 70. Boguth CA, Singh P, Huang C, Tesmer JJG. Molecular basis for activation of G protein-coupled
798 receptor kinases. EMBO J. 2010;29: 3249–3259. doi:10.1038/emboj.2010.206

799 71. Huang C, Yoshino-Koh K, Tesmer JJG. A surface of the kinase domain critical for the allosteric
800 activation of G protein-coupled receptor kinases. J Biol Chem. 2009;284: 17206–17215.
801 doi:10.1074/jbc.M809544200

802 72. Huang C-C, Orban T, Jastrzebska B, Palczewski K, Tesmer JJG. Activation of G protein-coupled receptor
803 kinase 1 involves interactions between its N-terminal region and its kinase domain. Biochemistry
804 (Mosc). 2011;50: 1940–1949. doi:10.1021/bi101606e

805 73. Noble B, Kallal LA, Pausch MH, Benovic JL. Development of a yeast bioassay to characterize G protein-
806 coupled receptor kinases. Identification of an NH2-terminal region essential for receptor
807 phosphorylation. J Biol Chem. 2003;278: 47466–47476. doi:10.1074/jbc.M308257200

808 74. Pao CS, Benovic JL. Phosphorylation-independent desensitization of G protein-coupled receptors? Sci
809 STKE. 2002;2002: pe42. doi:10.1126/stke.2002.153.pe42

810 75. Sterne-Marr R, Tesmer JJG, Day PW, Stracquatanio RP, Cilente J-AE, O'Connor KE, et al. G protein-
811 coupled receptor Kinase 2/G alpha q/11 interaction. A novel surface on a regulator of G protein
812 signaling homology domain for binding G alpha subunits. J Biol Chem. 2003;278: 6050–6058.
813 doi:10.1074/jbc.M208787200

814 76. Boekhoff I, Inglese J, Schleicher S, Koch WJ, Lefkowitz RJ, Breer H. Olfactory desensitization requires
815 membrane targeting of receptor kinase mediated by beta gamma-subunits of heterotrimeric G
816 proteins. J Biol Chem. 1994;269: 37–40.

817 77. Koch WJ, Inglese J, Stone WC, Lefkowitz RJ. The binding site for the beta gamma subunits of
818 heterotrimeric G proteins on the beta-adrenergic receptor kinase. J Biol Chem. 1993;268: 8256–8260.

819 78. Touhara K, Koch WJ, Hawes BE, Lefkowitz RJ. Mutational analysis of the pleckstrin homology domain
820 of the beta-adrenergic receptor kinase. Differential effects on G beta gamma and
821 phosphatidylinositol 4,5-bisphosphate binding. J Biol Chem. 1995;270: 17000–17005.

822 79. Carman CV, Barak LS, Chen C, Liu-Chen LY, Onorato JJ, Kennedy SP, et al. Mutational analysis of
823 Gbetagamma and phospholipid interaction with G protein-coupled receptor kinase 2. J Biol Chem.
824 2000;275: 10443–10452.

825 80. Topalidou I, Cattin-Ortolá J, Pappas AL, Cooper K, Merrihew GE, MacCoss MJ, et al. The EARP Complex
826 and Its Interactor EIPR-1 Are Required for Cargo Sorting to Dense-Core Vesicles. PLoS Genet. 2016;12:
827 e1006074. doi:10.1371/journal.pgen.1006074

828 81. Hammarlund M, Palfreyman MT, Watanabe S, Olsen S, Jorgensen EM. Open syntaxin docks synaptic
829 vesicles. PLoS Biol. 2007;5: e198. doi:10.1371/journal.pbio.0050198

830 82. Koelle MR. Neurotransmitter signaling through heterotrimeric G proteins: insights from studies in C.
831 elegans. WormBook Online Rev C Elegans Biol. 2016; 1–78. doi:10.1895/wormbook.1.75.2

832 83. Bastiani CA, Gharib S, Simon MI, Sternberg PW. Caenorhabditis elegans Galphaq regulates egg-laying
833 behavior via a PLCbeta-independent and serotonin-dependent signaling pathway and likely functions
834 both in the nervous system and in muscle. Genetics. 2003;165: 1805–1822.

835 84. Brundage L, Avery L, Katz A, Kim UJ, Mendel JE, Sternberg PW, et al. Mutations in a C. elegans
836 Gqalpha gene disrupt movement, egg laying, and viability. Neuron. 1996;16: 999–1009.

837 85. Mendel JE, Korswagen HC, Liu KS, Hajdu-Cronin YM, Simon MI, Plasterk RH, et al. Participation of the
838 protein Go in multiple aspects of behavior in C. elegans. Science. 1995;267: 1652–1655.

839 86. Ségalat L, Elkes DA, Kaplan JM. Modulation of serotonin-controlled behaviors by Go in Caenorhabditis
840 elegans. Science. 1995;267: 1648–1651.

841 87. Hajdu-Cronin YM, Chen WJ, Patikoglou G, Koelle MR, Sternberg PW. Antagonism between G(o)alpha
842 and G(q)alpha in Caenorhabditis elegans: the RGS protein EAT-16 is necessary for G(o)alpha signaling
843 and regulates G(q)alpha activity. Genes Dev. 1999;13: 1780–1793.

844 88. Nurrish S, Ségalat L, Kaplan JM. Serotonin inhibition of synaptic transmission: Galpha(0) decreases the
845 abundance of UNC-13 at release sites. Neuron. 1999;24: 231–242.

846 89. Sawin ER, Ranganathan R, Horvitz HR. C. elegans locomotory rate is modulated by the environment
847 through a dopaminergic pathway and by experience through a serotonergic pathway. Neuron.
848 2000;26: 619–631.

849 90. Lints R, Emmons SW. Patterning of dopaminergic neurotransmitter identity among Caenorhabditis
850 elegans ray sensory neurons by a TGFbeta family signaling pathway and a Hox gene. Development.
851 1999;126: 5819–5831.

852 91. Xie L, Gao S, Alcaire SM, Aoyagi K, Wang Y, Griffin JK, et al. NLF-1 delivers a sodium leak channel to
853 regulate neuronal excitability and modulate rhythmic locomotion. Neuron. 2013;77: 1069–1082.
854 doi:10.1016/j.neuron.2013.01.018

855 92. Koelle MR, Horvitz HR. EGL-10 regulates G protein signaling in the C. elegans nervous system and
856 shares a conserved domain with many mammalian proteins. Cell. 1996;84: 115–125.

857 93. Stefanakis N, Carrera I, Hobert O. Regulatory Logic of Pan-Neuronal Gene Expression in C. elegans.
858 Neuron. 2015;87: 733–750. doi:10.1016/j.neuron.2015.07.031

859 94. Zhang F, Bhattacharya A, Nelson JC, Abe N, Gordon P, Lloret-Fernandez C, et al. The LIM and POU
860 homeobox genes ttx-3 and unc-86 act as terminal selectors in distinct cholinergic and serotonergic
861 neuron types. Development. 2014;141: 422–435. doi:10.1242/dev.099721

862 95. Wenick AS, Hobert O. Genomic cis-regulatory architecture and trans-acting regulators of a single
863 interneuron-specific gene battery in C. elegans. Dev Cell. 2004;6: 757–770.
864 doi:10.1016/j.devcel.2004.05.004

865 96. Ezak MJ, Ferkey DM. The C. elegans D2-like dopamine receptor DOP-3 decreases behavioral
866 sensitivity to the olfactory stimulus 1-octanol. PloS One. 2010;5: e9487.
867 doi:10.1371/journal.pone.0009487

868 97. Ferkey DM, Hyde R, Haspel G, Dionne HM, Hess HA, Suzuki H, et al. C. elegans G protein regulator
869 RGS-3 controls sensitivity to sensory stimuli. Neuron. 2007;53: 39–52.
870 doi:10.1016/j.neuron.2006.11.015

871 98. Wragg RT, Hapiak V, Miller SB, Harris GP, Gray J, Komuniecki PR, et al. Tyramine and octopamine
872 independently inhibit serotonin-stimulated aversive behaviors in Caenorhabditis elegans through two
873 novel amine receptors. J Neurosci. 2007;27: 13402–13412. doi:10.1523/JNEUROSCI.3495-07.2007

874 99. Shiina T, Arai K, Tanabe S, Yoshida N, Haga T, Nagao T, et al. Clathrin box in G protein-coupled
875 receptor kinase 2. J Biol Chem. 2001;276: 33019–33026. doi:10.1074/jbc.M100140200

876 100. Namkung Y, Dipace C, Urizar E, Javitch JA, Sibley DR. G protein-coupled receptor kinase-2
877 constitutively regulates D2 dopamine receptor expression and signaling independently of receptor
878 phosphorylation. J Biol Chem. 2009;284: 34103–34115. doi:10.1074/jbc.M109.055707

879 101. Daigle TL, Ferris MJ, Gainetdinov RR, Sotnikova TD, Urs NM, Jones SR, et al. Selective deletion of GRK2
880 alters psychostimulant-induced behaviors and dopamine neurotransmission.
881 Neuropsychopharmacology. 2014;39: 2450–2462. doi:10.1038/npp.2014.97

882 102. Miller KG, Emerson MD, Rand JB. Goalpha and diacylglycerol kinase negatively regulate the Gqalpha
883 pathway in C. elegans. Neuron. 1999;24: 323–333.

884 103. Lackner MR, Nurrish SJ, Kaplan JM. Facilitation of synaptic transmission by EGL-30 Gqalpha and EGL-8
885 PLCbeta: DAG binding to UNC-13 is required to stimulate acetylcholine release. Neuron. 1999;24:
886 335–346.

887 104. Chalfie M, Sulston JE, White JG, Southgate E, Thomson JN, Brenner S. The neural circuit for touch
888 sensitivity in Caenorhabditis elegans. J Neurosci. 1985;5: 956–964.

889 105. Zheng Y, Brockie PJ, Mellem JE, Madsen DM, Maricq AV. Neuronal control of locomotion in C. elegans
890 is modified by a dominant mutation in the GLR-1 ionotropic glutamate receptor. Neuron. 1999;24:
891 347–361.

892 106. Brenner S. The genetics of Caenorhabditis elegans. Genetics. 1974;77: 71–94.

893 107. Hoyt JM, Wilson SK, Kasa M, Rise JS, Topalidou I, Ailion M. The SEK-1 p38 MAP Kinase Pathway
894 Modulates Gq Signaling in Caenorhabditis elegans. G3. 2017;[Epub ahead of print].
895 doi:10.1534/g3.117.043273

896 108. Frøkjær-Jensen C, Davis MW, Ailion M, Jorgensen EM. Improved Mos1-mediated transgenesis in C.
897 elegans. Nat Methods. 2012;9: 117–118. doi:10.1038/nmeth.1865

898 109. Mello CC, Kramer JM, Stinchcomb D, Ambros V. Efficient gene transfer in C.elegans:
899 extrachromosomal maintenance and integration of transforming sequences. EMBO J. 1991;10: 3959–
900 3970.

901 110. Pereira L, Kratsios P, Serrano-Saiz E, Sheftel H, Mayo AE, Hall DH, et al. A cellular and regulatory map
902 of the cholinergic nervous system of C. elegans. eLife. 2015;4: e12432. doi:10.7554/eLife.12432

903

904 **Figure Captions**

905 **Fig 1**. **The GRK-2 kinase regulates locomotion and G_q signaling.**

906 (A,B) *grk-2* mutations suppress activated G_q. The activated G_q mutant *egl-30(tg26)* (Gq*) has hyperactive
907 locomotion and a tightly coiled loopy posture. (A) The *grk-2(gk268)* and *grk-2(yak18)* mutations suppress
908 the loopy posture of activated G_q. (B) The *grk-2(gk268)* mutation suppresses the hyperactive locomotion of
909 activated G_q. (***, P<0.001. Error bars = SEM; n = 10).

910 (C) The kinase activity of GRK-2 is required for proper locomotion. The *grk-2(gk268)* and *grk-2(yak18)*
911 mutants have slow locomotion. The *grk-2(gk268)* slow locomotion is rescued by expression of the wild-
912 type *grk-2* cDNA under the control of its own promoter (GRK-2(+)), but is not rescued by expression of the
913 kinase dead GRK-2[K220R]. (**, P<0.01; ***, P<0.001. Error bars = SEM; n = 10-15).

914 (D) The kinase dead GRK-2 does not reverse the *grk-2* suppression of activated G_q. A *grk-2(gk268)*
915 mutation suppresses the hyperactive locomotion of *egl-30(tg26)* (Gq*). Expression of the kinase dead GRK-
916 2[K220R] does not rescue the *grk-2* mutant for this phenotype. (**, P<0.01. Error bars = SEM; n = 10).

917

918 **Fig 2. GRK-2 regulation of locomotion requires GPCR-phosphorylation and membrane association**.

919 (A) Domain structure of GRK-2. GRK-2 is a 707 amino acid protein with three well-characterized domains:
920 the RGS homology (RH) domain, the kinase domain, and the pleckstrin homology (PH) domain. The protein
921 structure was drawn using DOG 1.0.

922 (B-D) Residues required for GPCR phosphorylation are required for GRK-2 function in locomotion. The D3K
923 (transgene *yakEx77*), L4K (transgene *yakEx78*), V7A/L8A (transgene *yakEx79*), and D10A (transgene
924 *yakEx80*) mutations are predicted to block GPCR phosphorylation. The R195A mutation (transgene
925 *yakEx95*) disrupts predicted intramolecular stabilizing interactions that are required for effective
926 phosphorylation. In each case, expression of the mutant *grk-2* cDNA under the control of its own promoter

927 did not rescue the slow locomotion of the *grk-2(gk268)* mutant (ns, P>0.05, each strain compared to *grk-2*.
928 Error bars = SEM; n = 10-20).
929 (E) Residues in the RH domain predicted to disrupt G_q binding are not required for GRK-2 function in
930 locomotion. The R106A (transgene *yakEx57*), Y109I (transgene *yakEx55*), and D110A (transgene *yakEx56*)
931 mutations are predicted to disrupt G_q binding. In each case, expression of the mutant *grk-2* cDNA under
932 the control of the *grk-2* promoter significantly rescued the slow locomotion of the *grk-2(gk268)* mutant
933 (**, P<0.01; ***, P<0.001. Error bars = SEM; n = 10).
934 (F) Residues in the PH domain predicted to disrupt GRK-2 phospholipid binding or binding to Gβγ are
935 required for GRK-2 function in locomotion. Mutation K567E (transgene *yakEx87*) is predicted to disrupt
936 GRK-2 phospholipid binding, and mutation R587Q (transgene *yakEx88*) is predicted to disrupt binding to
937 Gβγ. In both cases, expression of the mutant *grk-2* cDNA under the control of the *grk-2* promoter did not
938 rescue the slow locomotion of the *grk-2(gk268)* mutant. (**, P<0.01. ns, P>0.05. Error bars = SEM; n = 10).
939 (G) Verification of the expression of the mutant *grk-2* cDNAs used for the experiments shown in Figure 1D
940 and Figure 2B-F. Western blot analysis of whole worm extracts from *grk-2(gk268)* mutants expressing the
941 indicated *grk-2* mutant cDNAs as extrachromosomal arrays.
942
943 **Fig 3. GRK-2 acts in head acetylcholine neurons.**
944 (A) *grk-2* acts in head acetylcholine neurons to control locomotion. The *grk-2* cDNA was expressed in *grk-*
945 *2(gk268)* mutants under a pan-neuronal promoter (*Prab-3,* transgene *yakEx44*), acetylcholine neuron
946 promoter (*Punc-17,* transgene *yakEx45*), ventral cord acetylcholine motor neuron promoter (*Pacr-2,*
947 transgene *yakEx47*), head acetylcholine neuron promoter (*Punc-17H,* transgene *yakEx51*), glutamate
948 receptor promoter (*Pglr-1,* transgene *yakEx52*), and ciliated sensory neuron promoter (*Pxbx-1,* transgene
949 *yakEx71*). Expression driven by the pan-neuronal, acetylcholine neuron, and head acetylcholine neuron
950 promoters rescued the slow locomotion of *grk-2* mutants. (***, P<0.001. Error bars = SEM; n = 10-25).

951 (B,C) GRK-2 acts in head acetylcholine neurons to positively regulate G_q signaling. A *grk-2(gk268)* mutant
952 suppresses the loopy posture and hyperactive locomotion of the activated G_q mutant *egl-30(tg26)* (Gq*).
953 Expression of the *grk-2* cDNA under a head acetylcholine neuron promoter (*Punc-17H*, transgene *yakEx51*)
954 reverses the *grk-2* suppression of the loopy posture (B) and hyperactive locomotion (C) of activated G_q.
955 (***, P<0.001. Error bars = SEM; n = 10).
956 (D) *grk-2* is expressed in head acetylcholine neurons. Representative images of a Z-stack projection of the
957 area around the nerve ring in the head of an animal coexpressing tagRFP fused to the GRK-2 ORF driven by
958 the *grk-2* promoter (*grk-2*::tagRFP, integration *yakIs19*) and GFP under a head acetylcholine neuron
959 promoter (*Punc-17H*::eGFP, transgene *yakEx94*). Anterior to the left. Because *Punc-17H*::GFP is highly
960 expressed and diffuse throughout the cell but *grk-2*::tagRFP is dimmer and localized only in the cytoplasm,
961 their coexpression is hard to see in the merged image. For this reason, we have circled the cells where
962 there is coexpression. Scale bar: 10 µm.
963
964 **Fig 4. Mutations in *dop-3* and *cat-2* suppress *grk-2*.**
965 (A) Mutations in *dop-3* and *cat-2* suppress the slow locomotion of *grk-2* mutants. The *grk-2(gk268)* mutant
966 has a slow locomotion phenotype. The *dop-3(vs106)* mutation fully suppresses and the *cat-2(e1112)*
967 mutation partially suppresses the slow locomotion of the *grk-2(gk268)* mutant (***, P<0.001. Error bars =
968 SEM; n = 32-72).
969 (B,C) A *dop-3* mutation reverses the *grk-2* mutant suppression of activated G_q. The *grk-2(gk268)* mutation
970 suppresses the loopy posture and hyperactive locomotion of the activated G_q mutant *egl-30(tg26)* (Gq*).
971 The *dop-3(vs106)* mutation reverses the *grk-2* suppression of the loopy posture (B) and hyperactive
972 locomotion (C) of Gq*. (***, P<0.001. Error bars = SEM; n = 15-20).
973 (D,E) *dop-3* and *cat-2* mutations reverse the *grk-2* mutant suppression of the loopy posture of activated
974 G_q. The *grk-2(gk268)* mutation suppresses the loopy posture of the activated G_q mutant *egl-30(tg26)*

975 (Gq*).The *dop-3 (vs106)* and *cat-2(e1112)* mutations reverse the *grk-2* suppression of the loopy posture of
976 Gq*. (***, P<0.001. ns, P>0.05. Error bars = SEM; n = 5).
977 (F) *grk-2* mutants are hypersensitive to dopamine in a *dop-3*-dependent manner. Shown is the percentage
978 of wild type, *dop-3(vs106), grk-2(gk268),* or *grk-2(gk268); dop-3(vs106)* animals that moved ten body
979 bends after a 20 min exposure to the indicated concentrations of dopamine. Every data point represents
980 the mean +/- SEM of three trials (15-20 animals per experiment and strain).
981
982 **Fig 5. A *grk-2* mutation partially suppresses activated Rho but does not suppress activated NCA-1.**
983 (A,B) A *grk-2* mutation partially suppresses activated Rho. Animals expressing activated RHO-1 [RHO-
984 1[G14V]) under an acetylcholine promoter (Rho*, transgene *nzIs29*) have slow locomotion and loopy
985 posture. The *grk-2(gk268)* mutation partially suppresses both the loopy posture (A) and slow locomotion
986 (B) of the Rho* animals. (***, P<0.001. Error bars = SEM; n = 10).
987 (C,D) A *grk-2* mutation does not suppress activated NCA-1. The activated NCA-1 mutant (Nca*, *nca-*
988 *1(ox352)*) has slow locomotion and loopy posture. The *grk-2(gk268)* mutation does not suppress the loopy
989 posture (C) or the slow locomotion (D) of Nca*. To measure the locomotion of the slow moving Nca*
990 animals, we used a radial locomotion assay in which we placed animals in the center of a 10 cm plate and
991 measured how far the animals had moved in one hour. (ns, P>0.05. Error bars = SEM; n = 10).
992
993 **Fig 6. GRK-2 is a positive modulator of NCA-1 and NCA-2 channel activity.**
994 (A) A *grk-2* mutation enhances the weak forward fainting phenotype of an *nlf-1* mutant. Representative
995 images of wild-type, *nlf-1(tm3631),* and *grk-2(gk268); nlf-1(tm3631)* mutant animals. The asterisk shows
996 the anterior part of the worm that becomes straight when an animal faints.
997 (B) A *grk-2* mutation enhances the weak forward fainting phenotype of an *nlf-1* mutant. The *nlf-1(tm3631)*
998 mutant is a weak fainter. The *grk-2(gk268)* mutation enhances the *nlf-1* mutant so that the double is a

999 strong fainter. (***, P<0.001. Error bars = SEM; n = 10-20). The number shown is the number of body
1000 bends before the animal faints. If the animal made ten body bends without fainting, the assay was stopped
1001 and we recorded ten as the number (see Methods).
1002 (C) The *grk-2(gk268)* mutation enhances the *unc-73(ox317)* mutant so that the double mutant is a strong
1003 fainter. The *grk-2(gk268)* mutation has no effect on an *egl-8(sa47)* mutant. (***, P<0.001. Error bars =
1004 SEM; n = 15).
1005 (D) The *egl-10(md176)* mutation enhances the *nlf-1(tm3631)* mutant so that the double mutant is a strong
1006 fainter. (***, P<0.001. Error bars = SEM; n = 25).
1007 (E) Expression of activated G_o in head acetylcholine neurons inhibits locomotion. Animals expressing an
1008 activated G_o mutant (GOA-1[Q205L]) under a head acetylcholine neuron promoter (*Punc-17H*::GOA-1*,
1009 transgene *yakEx103*) move more slowly than wild type animals. (***, P<0.001. Error bars = SEM; n = 17).
1010 (F) Expression of activated G_o in head acetylcholine neurons enhances the weak forward fainting
1011 phenotype of an *nlf-1* mutant. The *nlf-1(tm3631)* mutant is a weak fainter in forward movement. The *nlf-*
1012 *1(tm3631)* mutant expressing an activated G_o mutant (GOA-1[Q205L]) under a head acetylcholine neuron
1013 promoter (*Punc-17H*::GOA-1*, transgene *yakEx103*) is a stronger fainter than the *nlf-1(tm3631)* mutant.
1014 (***, P<0.001. Error bars = SEM; n = 54).
1015
1016 **Fig 7. Dopamine negatively modulates NCA-1 and NCA-2 channel activity.**
1017 (A) The *cat-2(e1112)* mutation suppresses the weak forward fainting phenotype of the *nlf-1(tm3631)*
1018 mutant. (***, P<0.001. Error bars = SEM; n = 40).
1019 (B) The *dop-3(vs106)* mutation suppresses the weak forward fainting phenotype of the *nlf-1(tm3631)*
1020 mutant. (***, P<0.001. Error bars = SEM; n = 40).
1021 (C) The *dop-3(vs106)* mutation partially suppresses the strong forward fainting phenotype of the *grk-*
1022 *2(gk268)*; *nlf-1(tm3631)* double mutant. (***, P<0.001. Error bars = SEM; n = 40).

1023 (D) Exogenous dopamine causes the *grk-2(gk268)* mutant to faint in a *dop-3* dependent manner. Shown is
1024 the percentage of animals that faint within a period of ten body bends when moving backwards after
1025 exposure to 2 mM dopamine for 20 min. (***, P<0.001. Error bars = SEM; n = 2-5 trials of 14-25 animals
1026 each).
1027
1028 **Fig 8. GRK-2 is expressed and acts in command interneurons to regulate locomotion.**
1029 (A) *grk-2* is expressed in command interneurons. Representative images of a Z-stack projection of the area
1030 around the nerve ring (head) of an animal coexpressing tagRFP fused to the GRK-2 cDNA driven by the *grk-*
1031 *2* promoter (*grk-2::RFP*, transgene *yakIs19*) and a *cho-1* fosmid YFP reporter (*cho-1*^{fosmid}::SL2::YFP::H2B,
1032 transgene *otIs534*). For the *cho-1* fosmid reporter, an SL2-spliced, nuclear-localized *YFP::H2B* sequence
1033 was engineered right after the stop codon of the gene [93,110]. As indicated in the figure, *grk-2::RFP* is
1034 expressed in the AVA, AVB, AVD, and AVE command interneurons; SMD and RMD head motor neurons;
1035 and in the AIN, AIY, SIA, SIB, and SAA interneurons. Scale bar: 10 µm.
1036 (B-D) *grk-2* cDNA expression in (B) SMD/RMD (*Pcho-1,* 3.3 to 2.6 kb upstream of the ATG, transgene
1037 *yakEx135*), (C) SIA/SIB (*Pceh-24*, transgene *yakEx149*), or (D) AIY (*Pttx-3*, transgene *yakEx138*) neurons
1038 does not rescue the slow locomotion of *grk-2(gk268)* mutants. (Error bars = SEM; n = 15).
1039 (E) *grk-2* cDNA expression in command interneurons (*Psra-11 + Pnmr-1*, transgene *yakEx141*) is sufficient
1040 to rescue the slow locomotion of *grk-2(gk268)* mutants. (***, P<0.001. Error bars = SEM; n = 25).
1041 (F) *grk-2* cDNA expression in command interneurons (*Psra-11 + Pnmr-1*, transgene *yakEx141*) is sufficient
1042 to rescue the strong fainting phenotype of *grk-2(gk268); nlf-1(tm3631)* mutants. (***, P<0.001. Error bars
1043 = SEM; n = 40).
1044 (G) *dop-3* cDNA expression in command interneurons (*Psra-11 + Pnmr-1*, transgene *yakEx148*) is sufficient
1045 to reverse the *dop-3(vs106)* mutant suppression of the slow locomotion of *grk-2(gk268)* mutant animals.
1046 (**, P<0.01. Error bars = SEM; n = 23).

1047

1048 **Fig 9. Model for GRK-2 and dopamine action in modulating activity of the NCA channels.**

1049 Schematic representation of the dopamine, G_q and G_o signaling pathways [61,82]. Solid arrows indicate

1050 direct actions or direct physical interactions. Dashed arrows indicate interactions that may be indirect. Our

1051 results suggest that dopamine decreases activity of the NCA-1 and NCA-2 channels (shown here

1052 collectively as "NCA") by binding to DOP-3 and activating G_o signaling. GRK-2 acts as a kinase for the D2-

1053 like dopamine receptor DOP-3 to inhibit DOP-3, and thereby inhibit G_o, activate G_q, and positively regulate

1054 NCA-1 and NCA-2 channel activity.

1055 **Supporting information**

1056 **S1 Fig. *grk-2* mutant phenotypes.**

1057 (A) The *grk-2(gk268)* mutant has an egg-laying defect. The graph shows the number of eggs laid by 5

1058 animals in a 2 h period. (**, P<0.01. Error bars = SEM; n = 2 plates of 5 animals each).

1059 (B) The *grk-2(gk268)* mutant animals have short bodies. (***, P<0.001. Error bars = SEM; n = 10).

1060 (C) A *dop-3* mutation does not suppress the restricted exploration behavior of *grk-2* mutants. Shown are

1061 images of tracks of five wild-type, *grk-2(gk268),* and *grk-2(gk268); dop-3(vs106)* mutant animals that were

1062 allowed to explore a bacterial lawn for 2 hours at room temperature.

1063

1064 **S2 Fig. *grk-2* mutants have swimming defects.**

1065 Shown are plots of bending angle (midpoint) versus time for representative individual animals. The two

1066 plots of *grk-2(gk268)* mutant animals show individuals with strong and weak swimming defects. The *dop-*

1067 *3(vs106)* mutation suppresses the swimming defects of the *grk-2*(*gk268)* mutant.

1068

1069 **S3 Fig. Arrestin mutants do not have locomotion defects and do not suppress Gq*.**

1070 (A) The *arr-1(ok401)* mutant has no locomotion defect. (ns, P>0.05. Error bars = SEM; n = 10).

1071 (B) The *arr-1(ok401)* mutation does not suppress the loopy posture of the *egl-30(tg26)* mutant.

1072 (C) The *arr-1(ok401)* mutation, in contrast to a *grk-2(gk268)* mutation, does not cause a fainting phenotype

1073 in an *nca-1(gk9)* mutant background. Shown is the percentage of animals that faint when moving

1074 backwards. The wild type, *nca-1*, *grk-2*, and *grk-2; nca-1* data are the same data shown in Figure S6F. The

1075 graph shows the combined data from two independent experiments, each with n = 20-40. (**, P<0.01;

1076 ***, P<0.001; ns, P>0.05).

1077

1078 **S4 Fig. A *grk-2* mutation suppresses the hyperactive locomotion of *dgk-1*, but not *goa-1* or *eat-16***

1079 **mutants.**

1080 (A) The *grk-2(gk268)* mutation does not suppress the hyperactive locomotion of the *eat-16(tm775)* and

1081 *goa-1(sa734)* mutants. (ns, P>0.05. Error bars = SEM; n = 10-20).

1082 (B) The *grk-2(gk268)* mutation suppresses the hyperactive locomotion phenotype of the *dgk-1(sy428)*

1083 mutant. (***, P<0.001. ns, P>0.05. Error bars = SEM; n = 10-20).

1084 (C-D) The *grk-2(gk268)* mutation does not suppress the loopy posture of the *eat-16(tm775)* and *goa-*

1085 *1(sa734)* mutants. (ns, P>0.05. Error bars = SEM; n = 5).

1086 (E) The kinase dead GRK-2 does not reverse the *grk-2* suppression of the *dgk-1* hyperactive locomotion

1087 phenotype. Expression of the kinase dead GRK-2[K220R] mutant under its own promoter (transgene

1088 *yakEx48*) does not reverse the *grk-2* suppression of *dgk-1* hyperactivity. (ns, P>0.05. Error bars = SEM; n =

1089 10-20).

1090 (F) Expression of the *grk-2* cDNA under a head acetylcholine neuron promoter (transgene *yakEx51*)

1091 reverses the *grk-2* suppression of the hyperactive locomotion of the *dgk-1(sy428)* mutant. (***, P<0.001.

1092 Error bars = SEM; n = 10-20).

1093

1094 **S5 Fig. A *cat-2* mutation reverses the *grk-2* mutant suppression of activated G_q.** The *grk-2(gk268)*

1095 mutation suppresses the loopy posture and hyperactive locomotion of the activated G_q mutant *egl-*

1096 *30(tg26)* (Gq*).The *cat-2(e1112)* mutation reverses the *grk-2* suppression of the loopy posture (A) and

1097 hyperactive locomotion (B) of Gq*. (***, P<0.001. Error bars = SEM; n = 15-20).

1098

1099 **S6 Fig. *dop-3* acts in head acetylcholine neurons to regulate *grk-2* dependent locomotion.**

1100 (A) The *dop-3* suppression of *grk-2* is reversed by *dop-3* expression in head acetylcholine neurons. The

1101 *dop-3* cDNA was expressed in the *grk-2(gk268); dop-3(vs106)* double mutant under a pan-neuronal

1102 promoter (*Prab-3,* transgene *yakEx112*), acetylcholine neuron promoter (*Punc-17,* transgene *yakEx111*),
1103 head acetylcholine neuron promoter (*Punc-17H,* transgene *yakEx110*) and ventral cord acetylcholine
1104 motor neuron promoter (*Pacr-2,* transgene *yakEx109*). Expression of *dop-3* driven by the pan-neuronal,
1105 acetylcholine neuron, and head acetylcholine neuron promoters reversed the *dop-3(vs106)* mutant
1106 suppression of the slow locomotion of *grk-2(gk268)* mutant animals. (*, P<0.05; **, P<0.01; ***, P<0.001;
1107 ns, P>0.05. Error bars = SEM; n = 10-33).
1108 (B) A *dop-1* mutation does not affect the *dop-3* suppression of the *grk-2* slow locomotion phenotype. *grk-*
1109 *2; dop-3* mutants move more rapidly than the *grk-2* mutant. The *dop-1(vs100)* mutation does not affect
1110 *grk-2(gk268); dop-3(vs106)* locomotion. (ns, P>0.05. Error bars = SEM; n = 23-34).
1111 (C-E) Expression of *dop-3* in ventral cord motor neurons is not sufficient to reverse the hyperactive
1112 locomotion and loopy posture of *egl-30(tg26); grk-2; dop-3* mutant animals. (C) Expression of *dop-3* driven
1113 by the ventral cord neuron promoter (*Pacr-2*, transgene *yakEx109*) does not reduce the hyperactivity of
1114 *egl-30(tg26); grk-2(gk268); dop-3(vs106)* mutant animals. (***, P<0.001; ns, P>0.05. Error bars = SEM; n =
1115 10). (D-E) Expression of *dop-3* driven by the ventral cord neuron promoter (*Pacr-2*, transgene *yakEx109*)
1116 does not reverse the loopy waveform of *egl-30(tg26); grk-2(gk268); dop-3(vs106)* mutant animals. (**,
1117 P<0.01; ***, P<0.001; ns, P>0.05. Error bars = SEM; n = 10).
1118 (F) A *dop-3* mutation suppresses the fainting phenotype of *grk-2; nca-1* mutants. Shown is the percentage
1119 of animals that faint when moving backwards. The wild type, *nca-1*, *grk-2*, and *grk-2; nca-1* data are the
1120 same data shown in Figure S3C. The graph shows the combined data from two independent experiments,
1121 each with n = 20-40. (**, P<0.01; ***, P<0.001; ns, P>0.05).
1122
1123 **S7 Fig. *grk-2* does not affect the level of expression or subcellular localization of DOP-3::GFP.**

1124 (A) DOP-3::GFP expression driven by the *grk-2* promoter (transgene *yakEx130*) reverses the *dop-3* mutant
1125 suppression of the slow locomotion phenotype of *grk-2* mutants. (**, P<0.01; ***, P<0.001. Error bars =
1126 SEM; n = 10).
1127 (B) DOP-3::GFP levels remain unaffected in *grk-2* mutants. Immunoblot of extracts derived from *dop-3* or
1128 *grk-2; dop-3* animals expressing *Pgrk-2*::DOP-3::GFP and *Pmyo-2*::mCherry from an extrachromosomal
1129 array (transgene *yakEx130*). The experiment was repeated twice with similar results.
1130 (C,D) DOP-3::GFP subcellular localization and level of expression remain unaffected in *grk-2* mutants. (C)
1131 Representative images of a Z-stack projection of the area around the nerve ring in the head of *dop-3* or
1132 *grk-2; dop-3* mutant animals expressing *Pgrk-2*::DOP-3::GFP (transgene *yakEx130*). (D) Quantification of
1133 the ratio of DOP-3::GFP to mCherry in the region around the nerve ring of *dop-3* or *grk-2; dop-3* animals
1134 expressing *Pgrk-2*::DOP-3::GFP and *Pmyo-2*::mCherry (transgene *yakEx130*). (ns, P>0.05. Error bars = SEM;
1135 n = 10).
1136
1137 **S8 Fig. Mutations in *dop-3* and *cat-2* do not suppress the strong fainter phenotype of *unc-80* mutants.**
1138 (A) The *dop-3(vs106)* mutation does not suppress the strong forward fainting phenotype of the *unc-*
1139 *80(ox330)* mutant. (ns, P>0.05. Error bars = SEM; n = 20).
1140 (B) The *cat-2(e1112)* mutation does not suppress the strong forward fainting phenotype of the *unc-*
1141 *80(ox330)* mutant. (ns, P>0.05. Error bars = SEM; n = 36-38).
1142
1143 **S9 Fig. *grk-2* expression driven by only the *sra-11* or *nmr-1* promoter does not rescue the slow**
1144 **locomotion of *grk-2* mutants.**
1145 (A), (B) *grk-2* cDNA expression driven by the (A) *sra-11* (*Psra-11*, transgene *yakEx147*) or (B) *nmr-1* (*Pnmr-*
1146 *1*, transgene *yakEx85*) promoter does not rescue the slow locomotion of the *grk-2(gk268)* mutant. (ns,
1147 P>0.05. Error bars = SEM; n = 10-20).

1148

1149

1150 **S1 Table. List of strains.**

1151

1152 **S2 Table. List of plasmids.**

1153

Fig 1

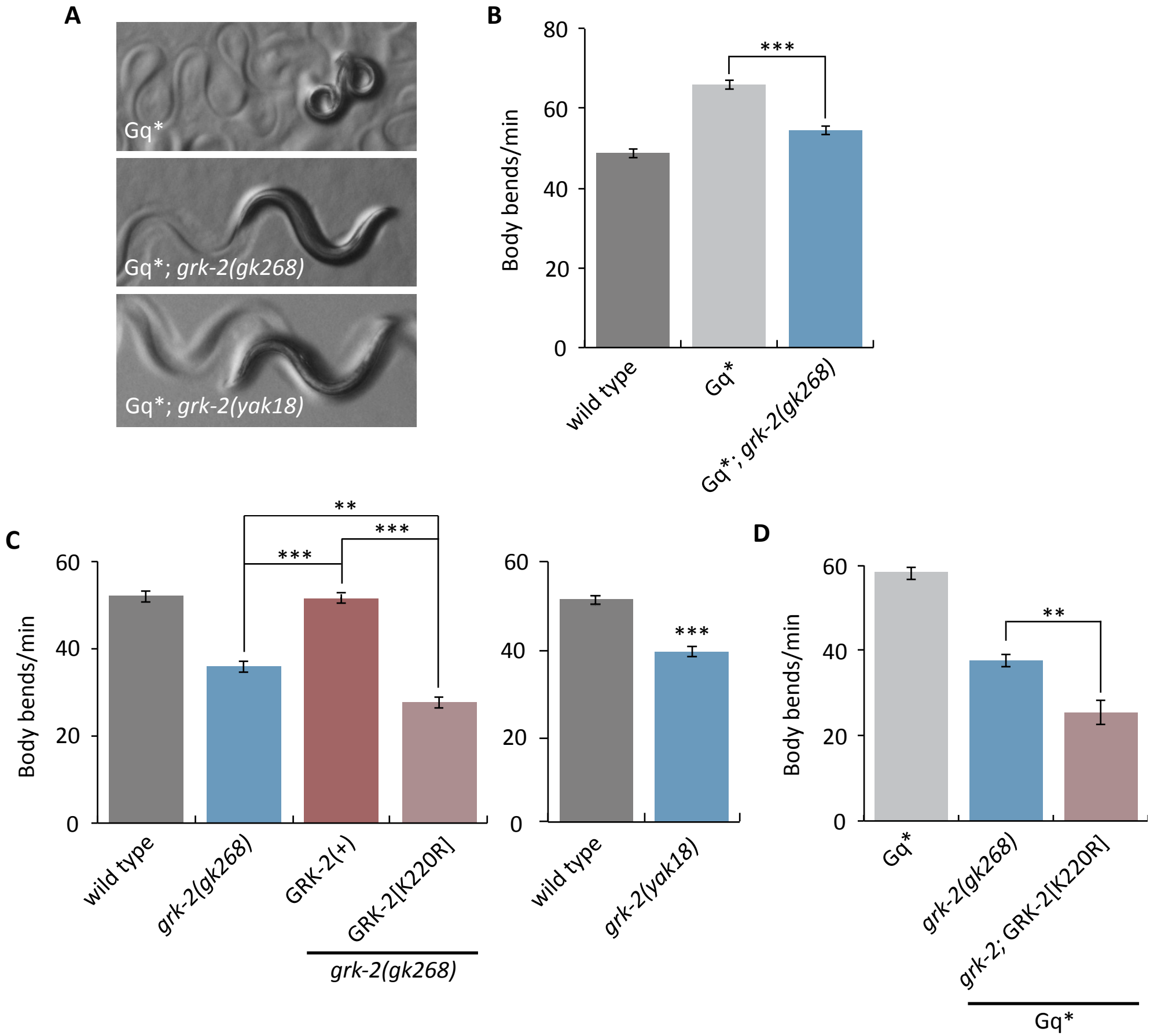
A
Gq*
Gq*; grk-2(gk268)
Gq*; grk-2(yak18)
B
Body bends/min
80
60
40
20
0
***
wild type
Gq*
Gq*; grk-2(gk268)
C
Body bends/min
60
40
20
0
**
***
***
wild type
grk-2(gk268)
GRK-2(+)
GRK-2[K220R]
grk-2(gk268)
60
40
20
0
***
wild type
grk-2(yak18)
D
Body bends/min
60
40
20
0
**
Gq*
grk-2(gk268)
grk-2; GRK-2[K220R]
Gq*

Fig 2

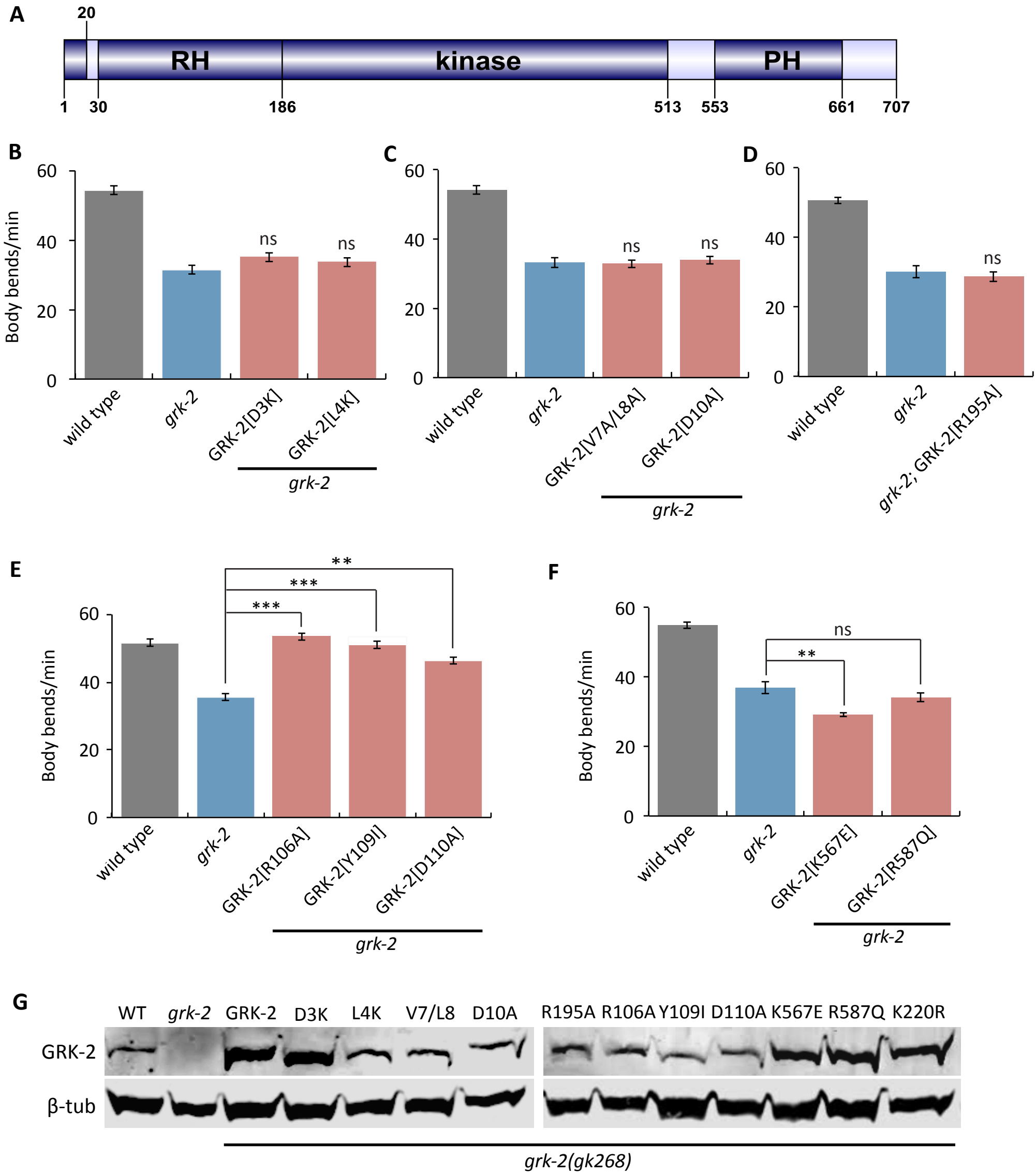
A
20
RH
kinase
PH
1
30
186
513
553
661
707
B
Body bends/min
60
40
20
0
ns
ns
wild type
grk-2
GRK-2[D3K]
GRK-2[L4K]
grk-2
C
60
40
20
0
ns
ns
wild type
grk-2
GRK-2[V7A/L8A]
GRK-2[D10A]
grk-2
D
60
40
20
0
ns
wild type
grk-2
grk-2; GRK-2[R195A]
E
Body bends/min
60
40
20
0
**
***
***
wild type
grk-2
GRK-2[R106A]
GRK-2[Y109I]
GRK-2[D110A]
grk-2
F
Body bends/min
60
40
20
0
ns
**
wild type
grk-2
GRK-2[K567E]
GRK-2[R587Q]
grk-2
G
WT
grk-2
GRK-2
D3K
L4K
V7/L8
D10A
R195A
R106A
Y109I
D110A
K567E
R587Q
K220R
GRK-2
β-tub
grk-2(gk268)

Fig 3

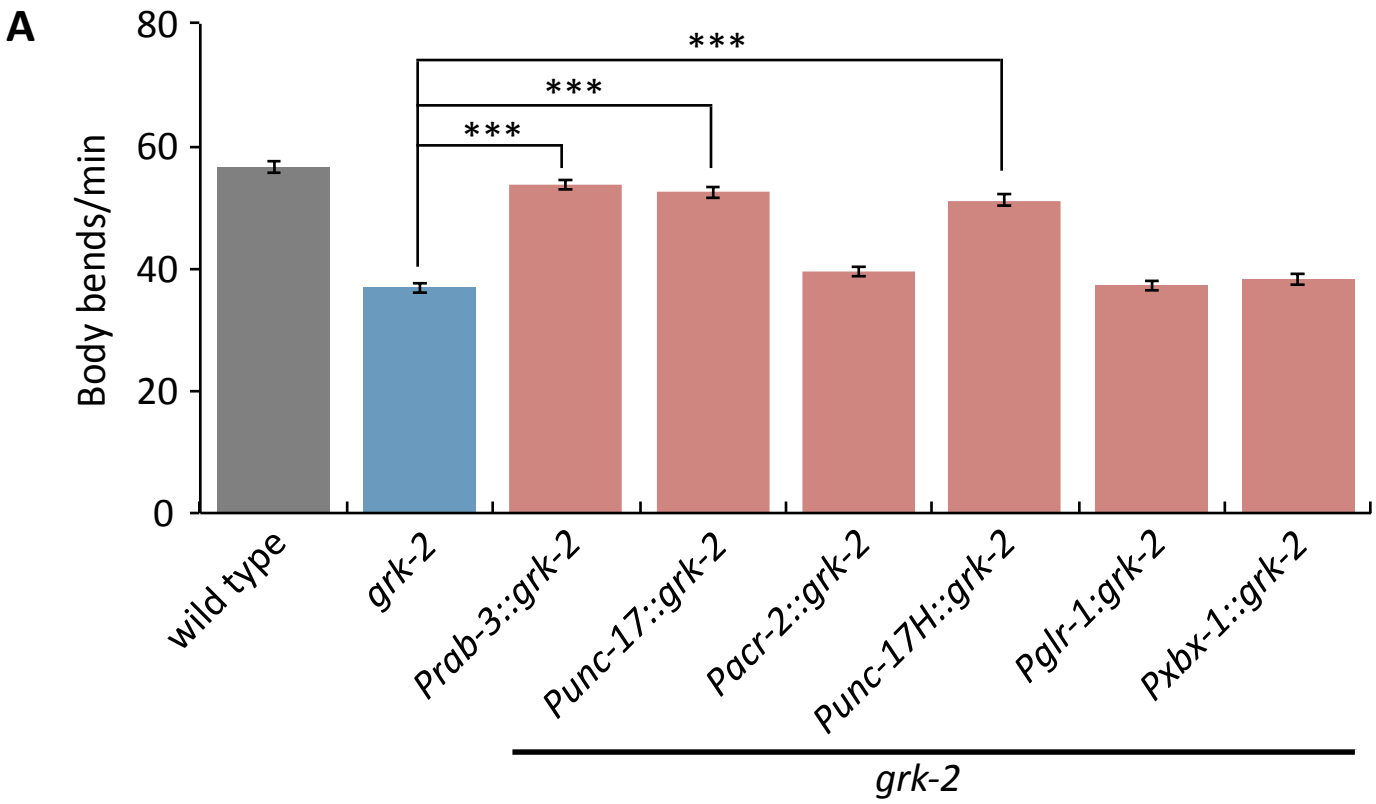
A
Body bends/min
80
60
40
20
0
***
***
***
wild type
grk-2
Prab-3::grk-2
Punc-17::grk-2
Pacr-2::grk-2
Punc-17H::grk-2
Pglr-1:grk-2
Pxbx-1::grk-2
grk-2

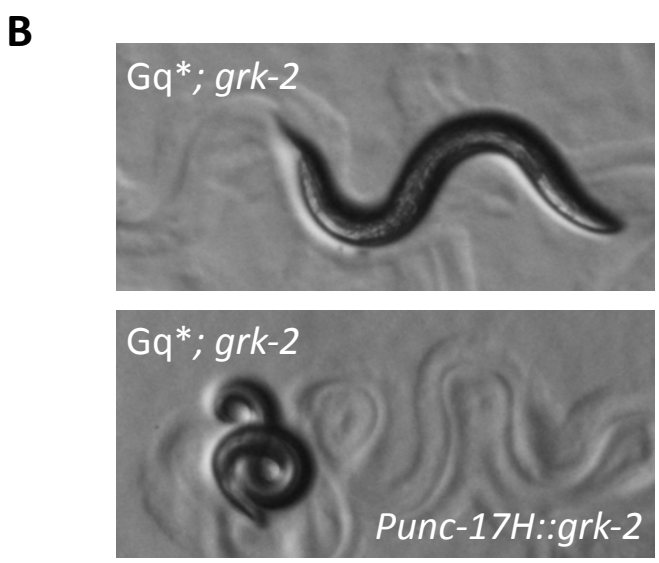
B
Gq*; grk-2
Gq*; grk-2
Punc-17H::grk-2

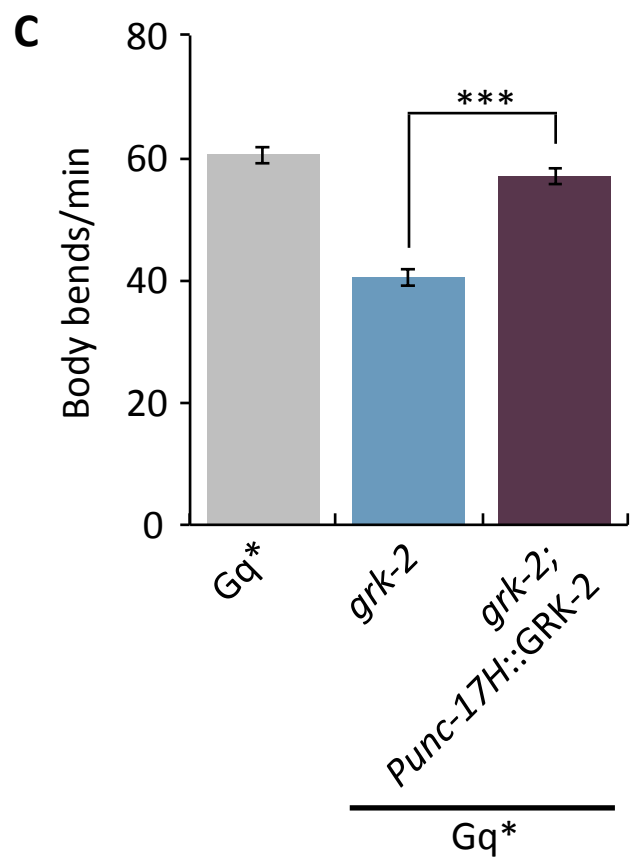
C
Body bends/min
80
60
40
20
0
***
Gq*
grk-2
grk-2;
Punc-17H::GRK-2
Gq*

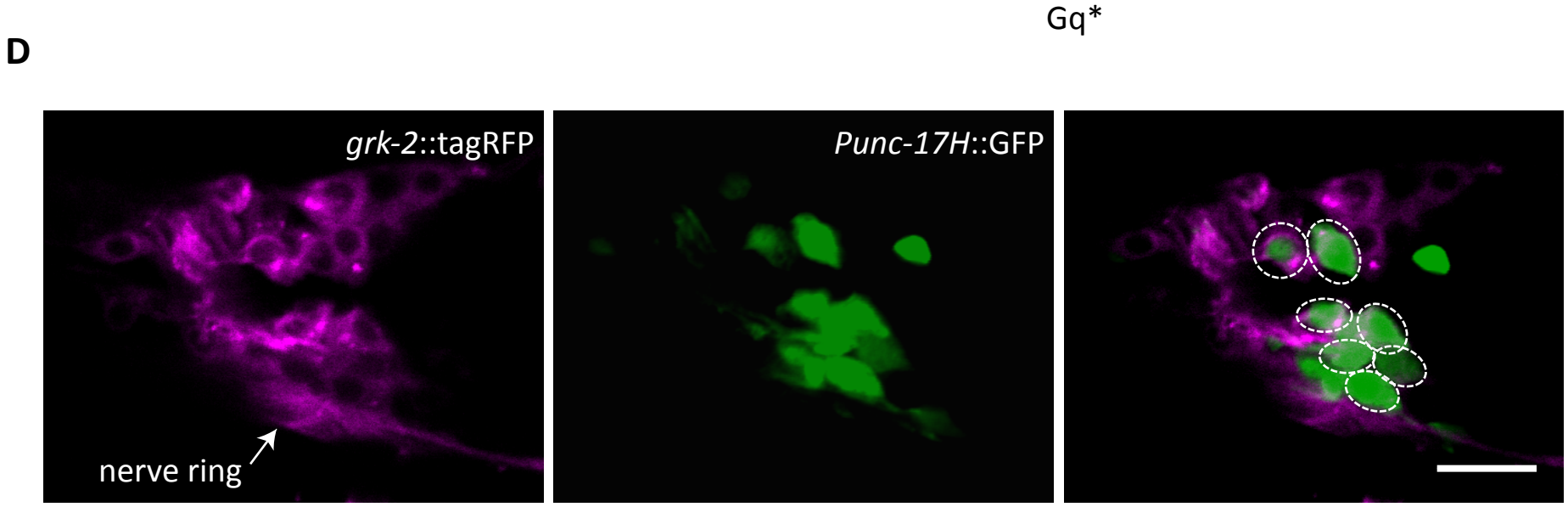
D
grk-2::tagRFP
nerve ring
Punc-17H::GFP

Fig 4

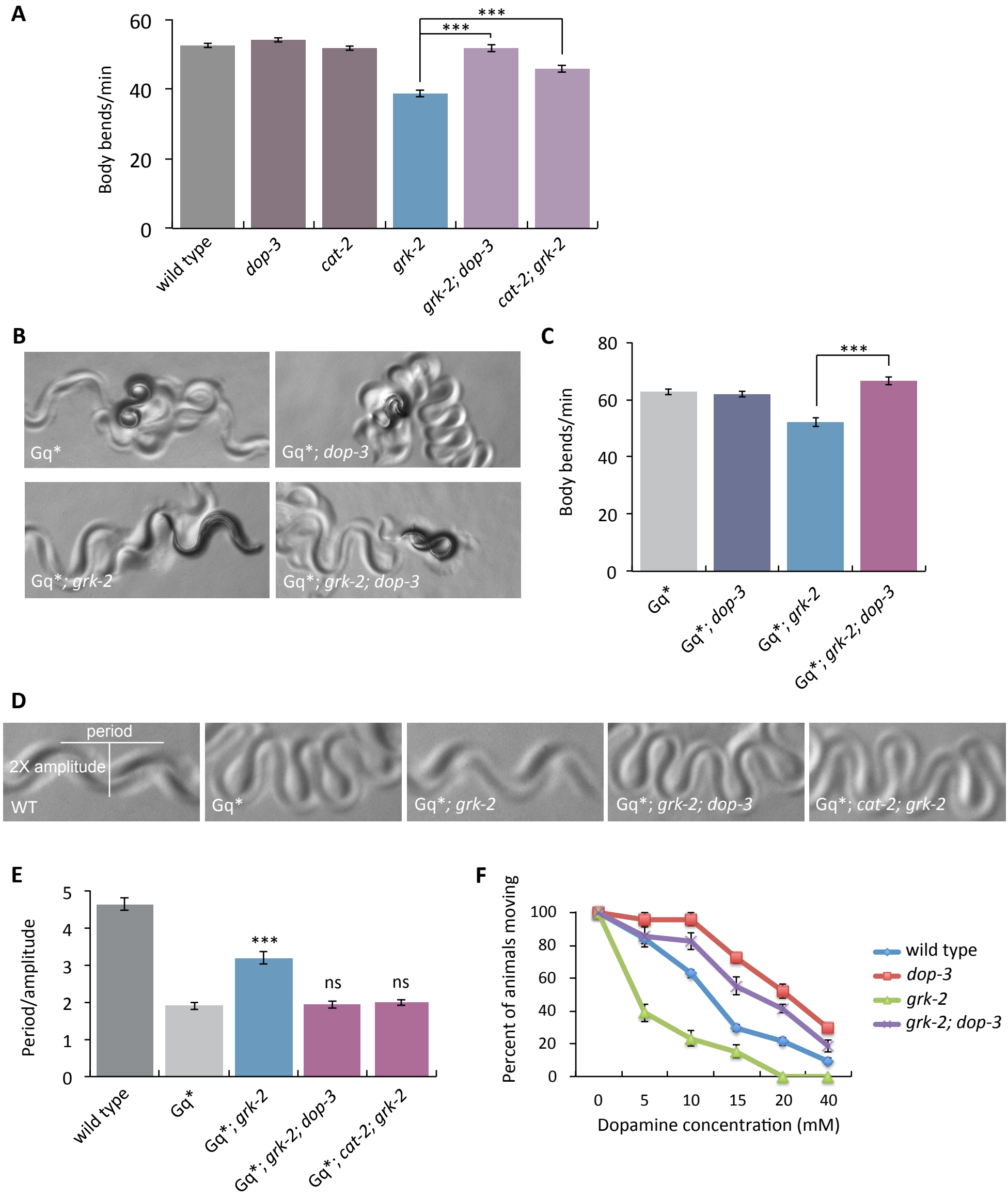
A
Body bends/min
60
40
20
0
***
***
wild type
dop-3
cat-2
grk-2
grk-2; dop-3
cat-2; grk-2
B
Gq*
Gq*; dop-3
Gq*; grk-2
Gq*; grk-2; dop-3
C
Body bends/min
80
60
40
20
0
***
Gq*
Gq*; dop-3
Gq*; grk-2
Gq*; grk-2; dop-3
D
period
2X amplitude
WT
Gq*
Gq*; grk-2
Gq*; grk-2; dop-3
Gq*; cat-2; grk-2
E
Period/amplitude
5
4
3
2
1
0
***
ns
ns
wild type
Gq*
Gq*; grk-2
Gq*; grk-2; dop-3
Gq*; cat-2; grk-2
F
Percent of animals moving
100
80
60
40
20
0
0
5
10
15
20
40
Dopamine concentration (mM)
wild type
dop-3
grk-2
grk-2; dop-3

Fig 5

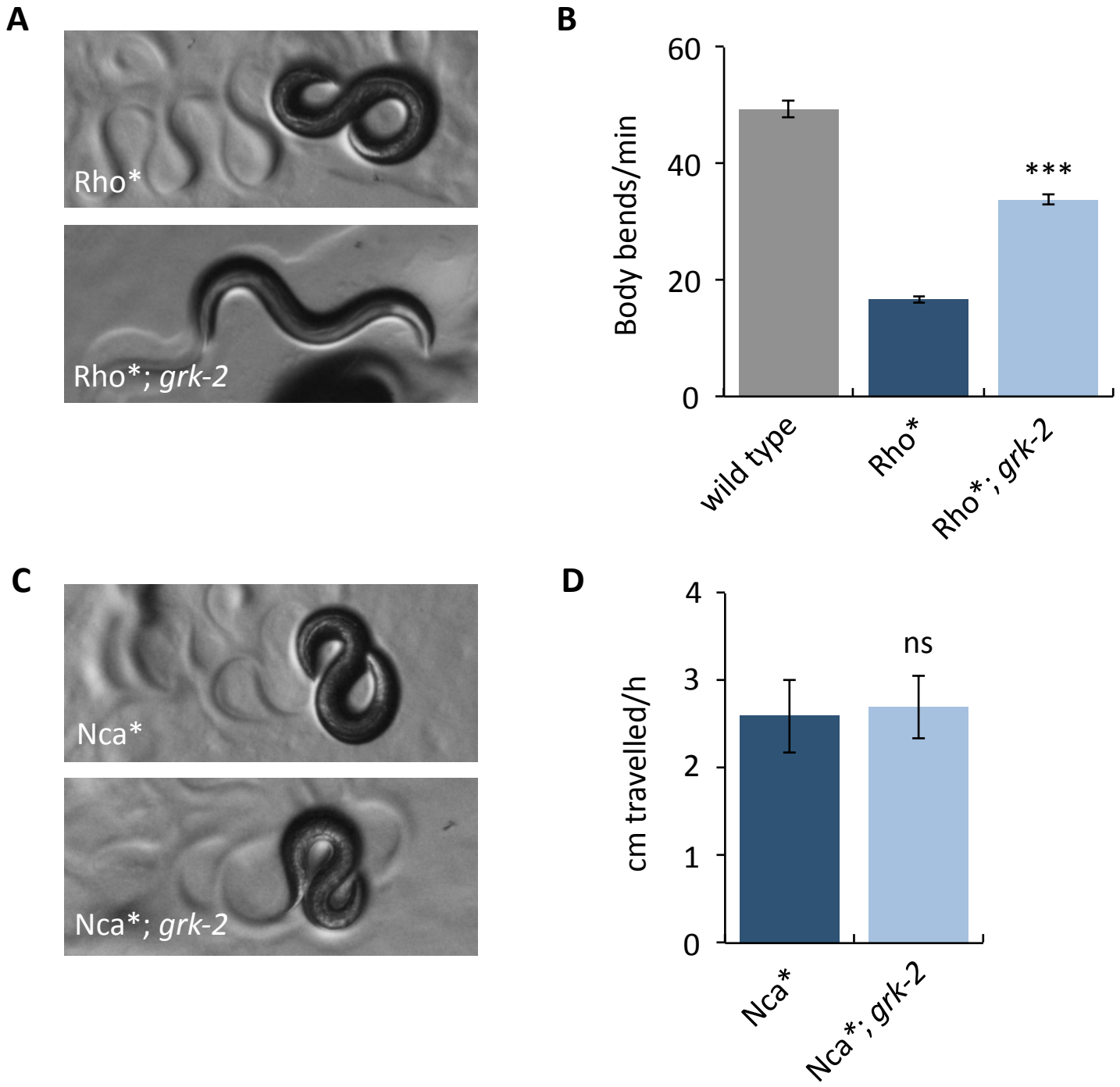
A
Rho*
Rho*; grk-2
B
Body bends/min
60
40
20
0
***
wild type
Rho*
Rho*; grk-2
C
Nca*
Nca*; grk-2
D
cm travelled/h
4
3
2
1
0
ns
Nca*
Nca*; grk-2

Fig 6

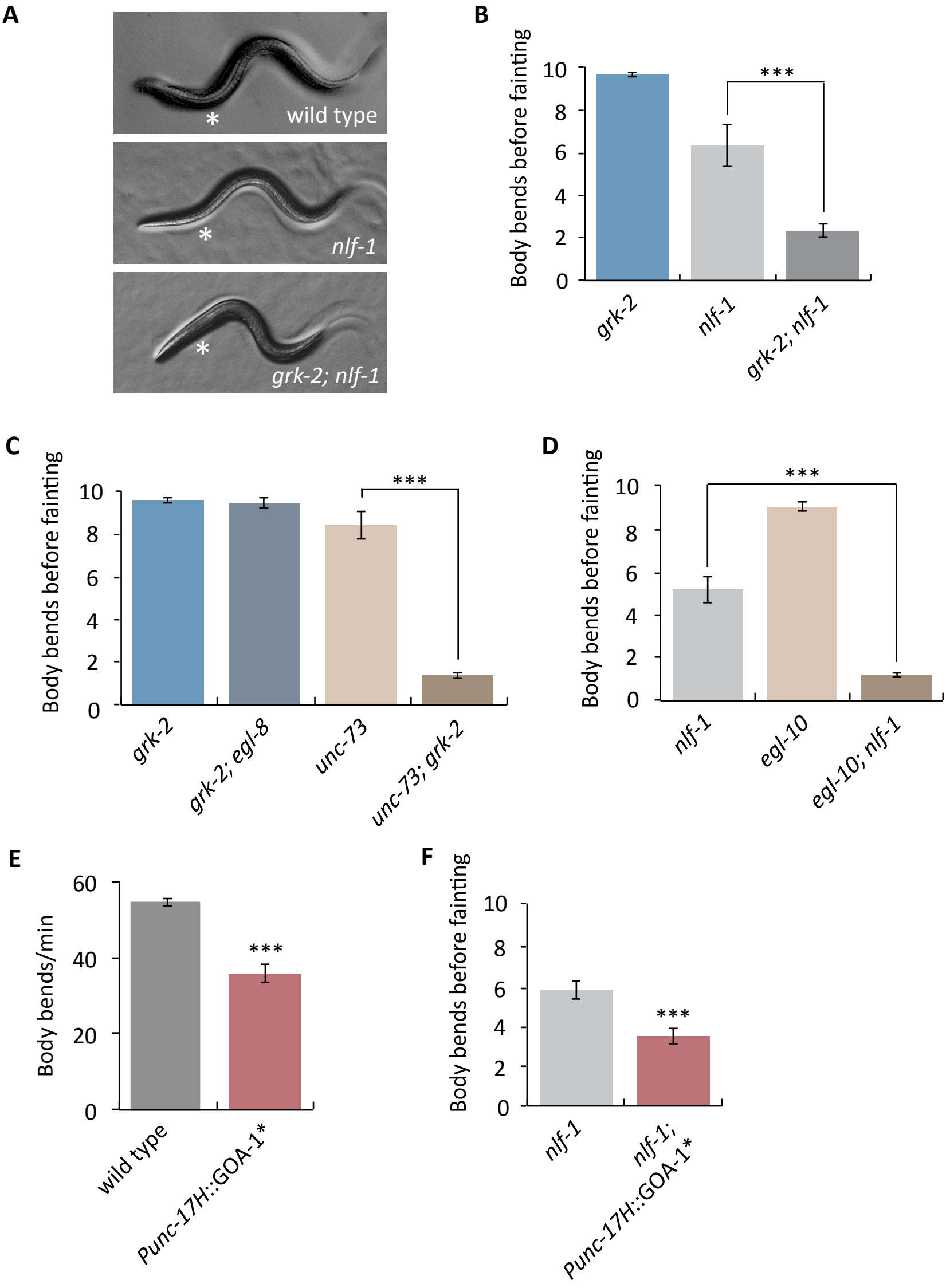
A
wild type
nlf-1
grk-2; nlf-1
B
Body bends before fainting
10
8
6
4
2
0
***
grk-2
nlf-1
grk-2; nlf-1
C
Body bends before fainting
10
8
6
4
2
0
***
grk-2
grk-2; egl-8
unc-73
unc-73; grk-2
D
Body bends before fainting
10
8
6
4
2
0
***
nlf-1
egl-10
egl-10; nlf-1
E
Body bends/min
60
40
20
0
***
wild type
Punc-17H::GOA-1*
F
Body bends before fainting
10
8
6
4
2
0
***
nlf-1
nlf-1;
Punc-17H::GOA-1*

Fig 7

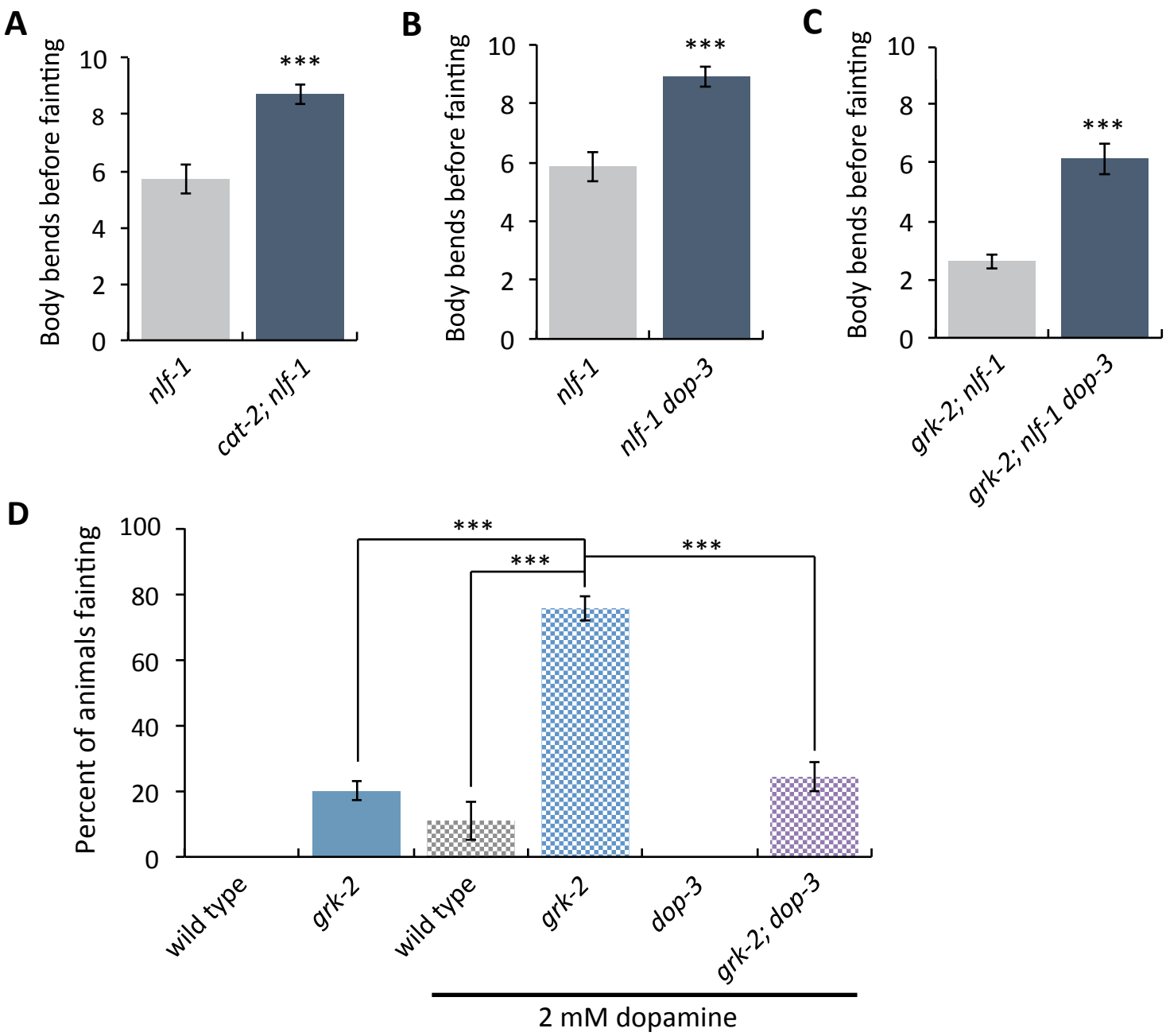
A
Body bends before fainting
10
8
6
4
2
0
***
nlf-1
cat-2; nlf-1
B
Body bends before fainting
10
8
6
4
2
0
***
nlf-1
nlf-1 dop-3
C
Body bends before fainting
10
8
6
4
2
0
***
grk-2; nlf-1
grk-2; nlf-1 dop-3
D
Percent of animals fainting
100
80
60
40
20
0
***
***
***
wild type
grk-2
wild type
grk-2
dop-3
grk-2; dop-3
2 mM dopamine

Fig 8

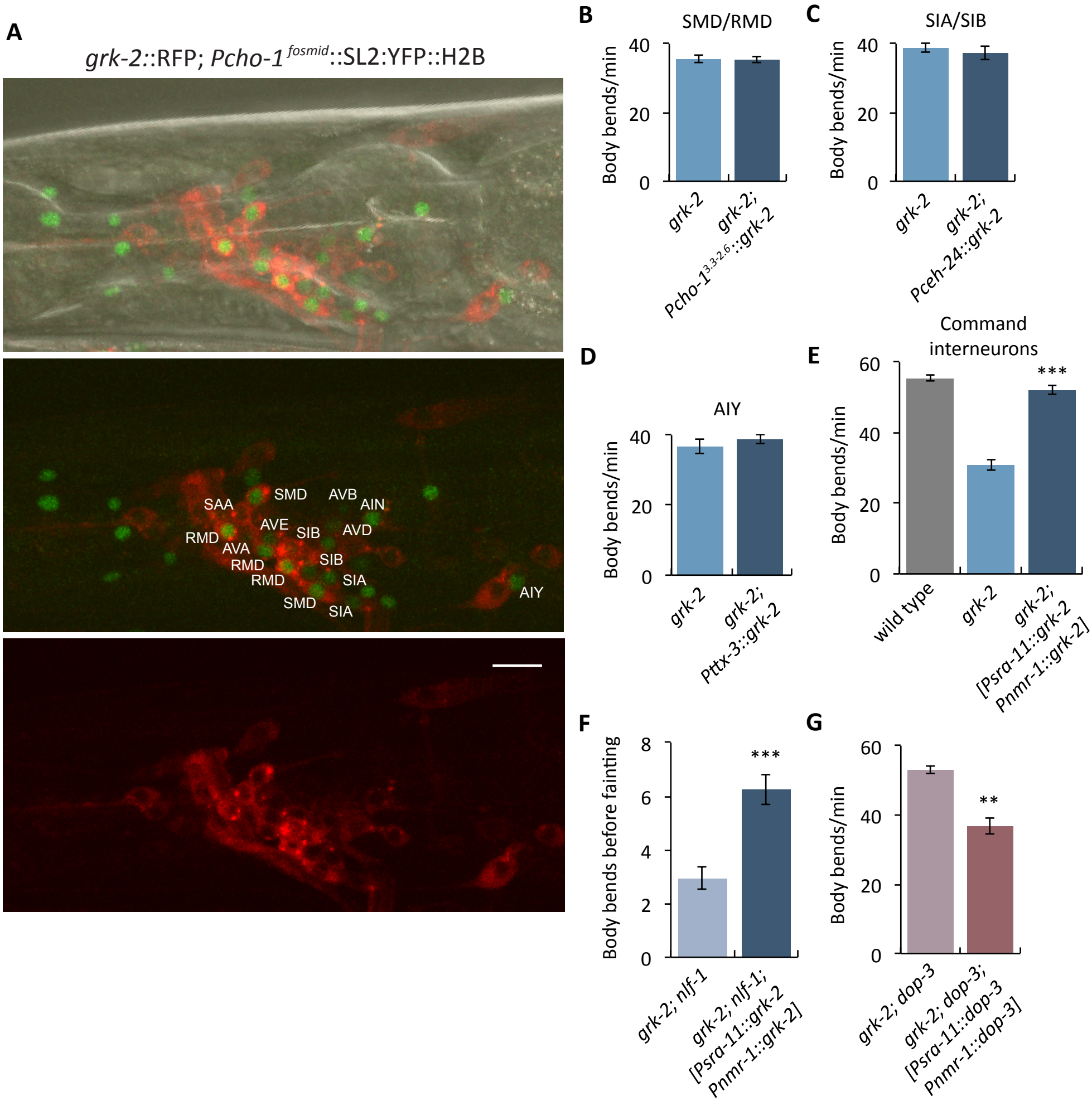
A
grk-2::RFP; Pcho-1 fosmid::SL2:YFP::H2B
SAA
SMD
AVB
AIN
AVE
SIB
AVD
RMD
AVA
RMD
SIB
RMD
SIA
SMD
SIA
AIY
B
SMD/RMD
Body bends/min
40
20
0
grk-2
grk-2; Pcho-1 3.3-2.6::grk-2
C
SIA/SIB
Body bends/min
40
20
0
grk-2
grk-2; Pceh-24::grk-2
D
AIY
Body bends/min
40
20
0
grk-2
grk-2; Pttx-3::grk-2
E
Command interneurons
Body bends/min
60
40
20
0
***
wild type
grk-2
grk-2; [Psra-11::grk-2 Pnmr-1::grk-2]
F
Body bends before fainting
8
6
4
2
0
***
grk-2; nlf-1
grk-2; nlf-1; [Psra-11::grk-2 Pnmr-1::grk-2]
G
Body bends/min
60
40
20
0
**
grk-2; dop-3
grk-2; dop-3; [Psra-11::dop-3 Pnmr-1::dop-3]

Fig 9

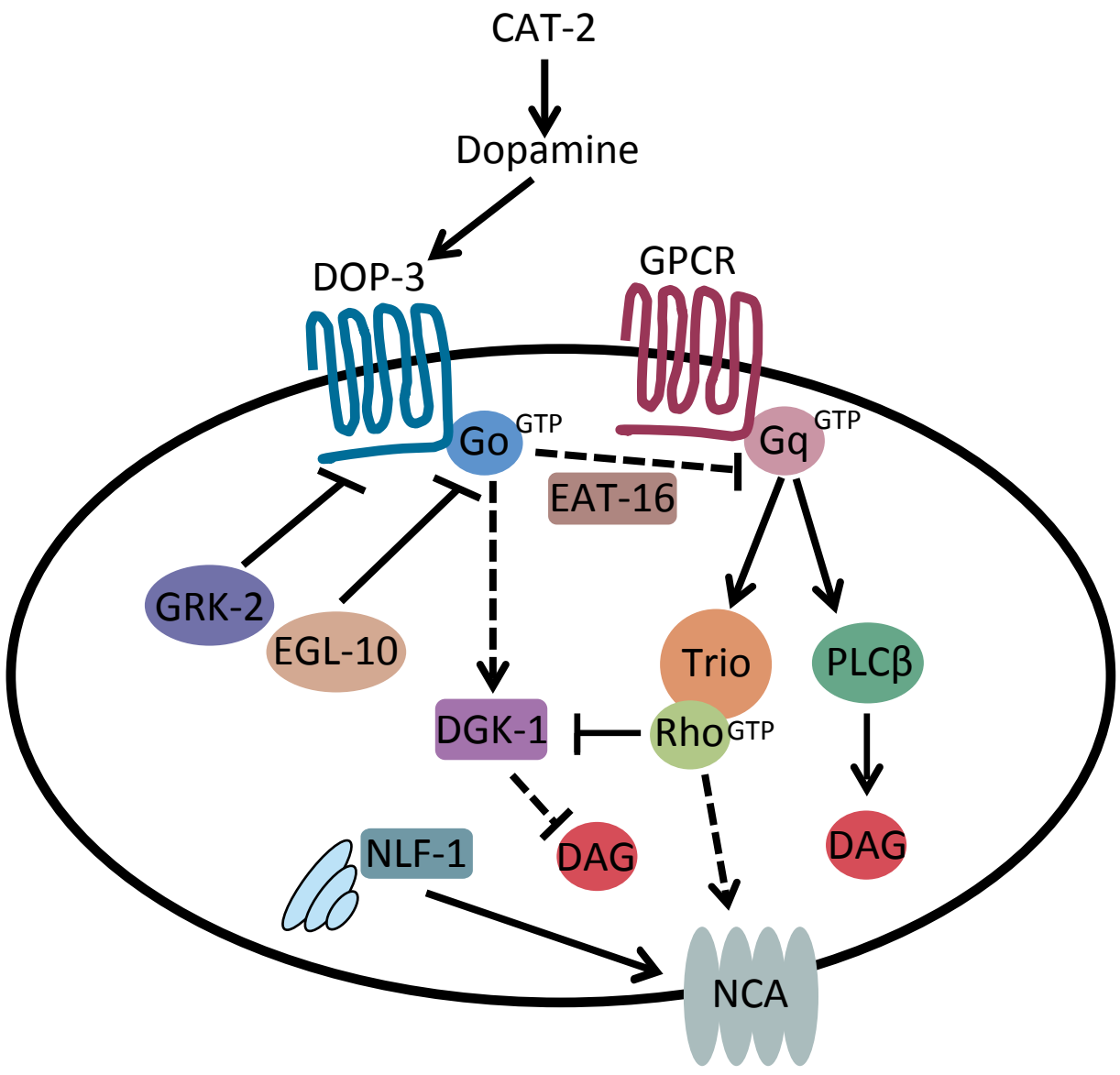
CAT-2
Dopamine
DOP-3
GPCR
Go
GTP
Gq
GTP
EAT-16
GRK-2
EGL-10
Trio
PLCβ
DGK-1
Rho
GTP
NLF-1
DAG
DAG
NCA

S1 Fig.

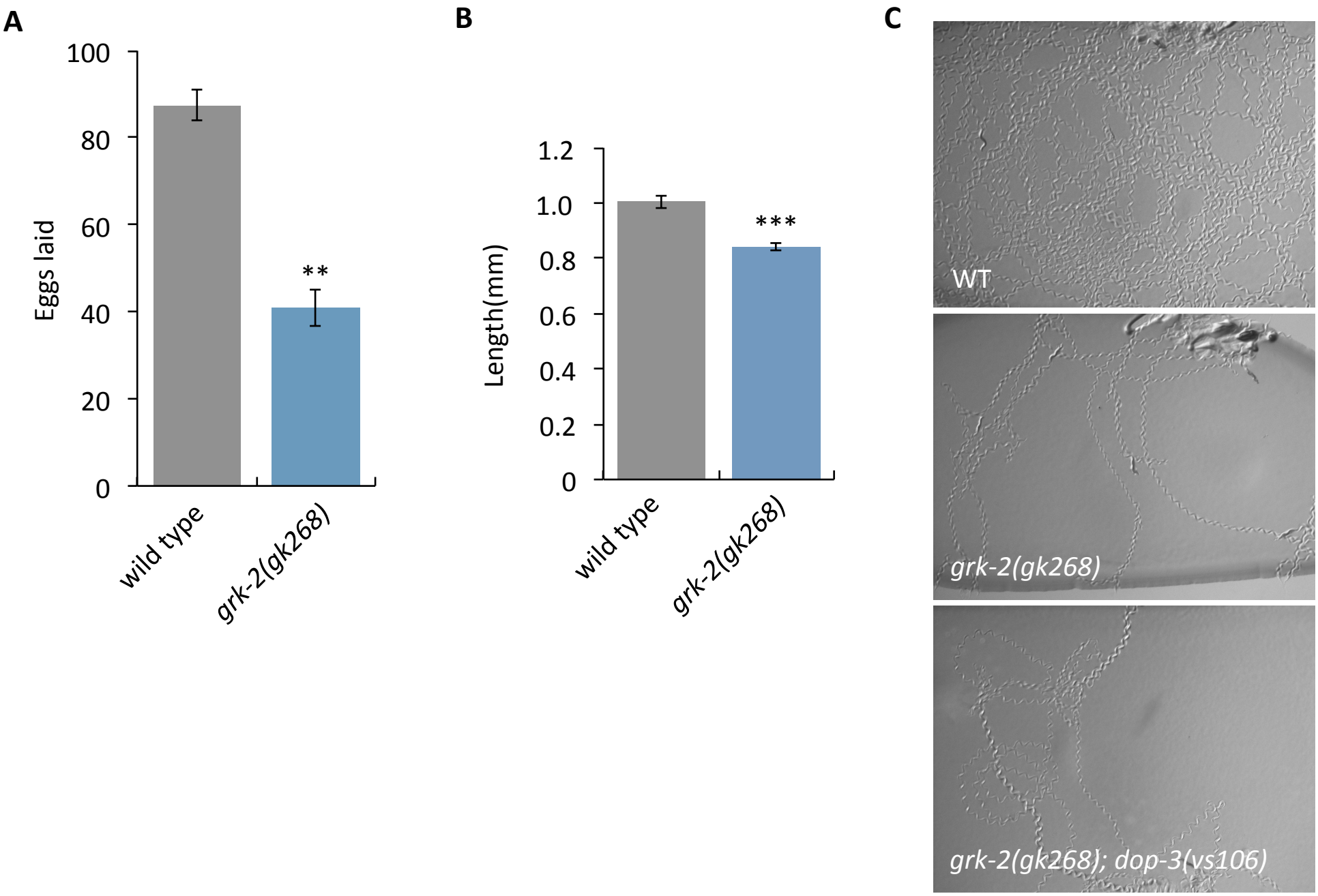
A
100
80
60
40
20
0
Eggs laid
**
wild type
grk-2(gk268)
B
1.2
1.0
0.8
0.6
0.4
0.2
0
Length(mm)
***
wild type
grk-2(gk268)
C
WT
grk-2(gk268)
grk-2(gk268); dop-3(vs106)

S2 Fig.

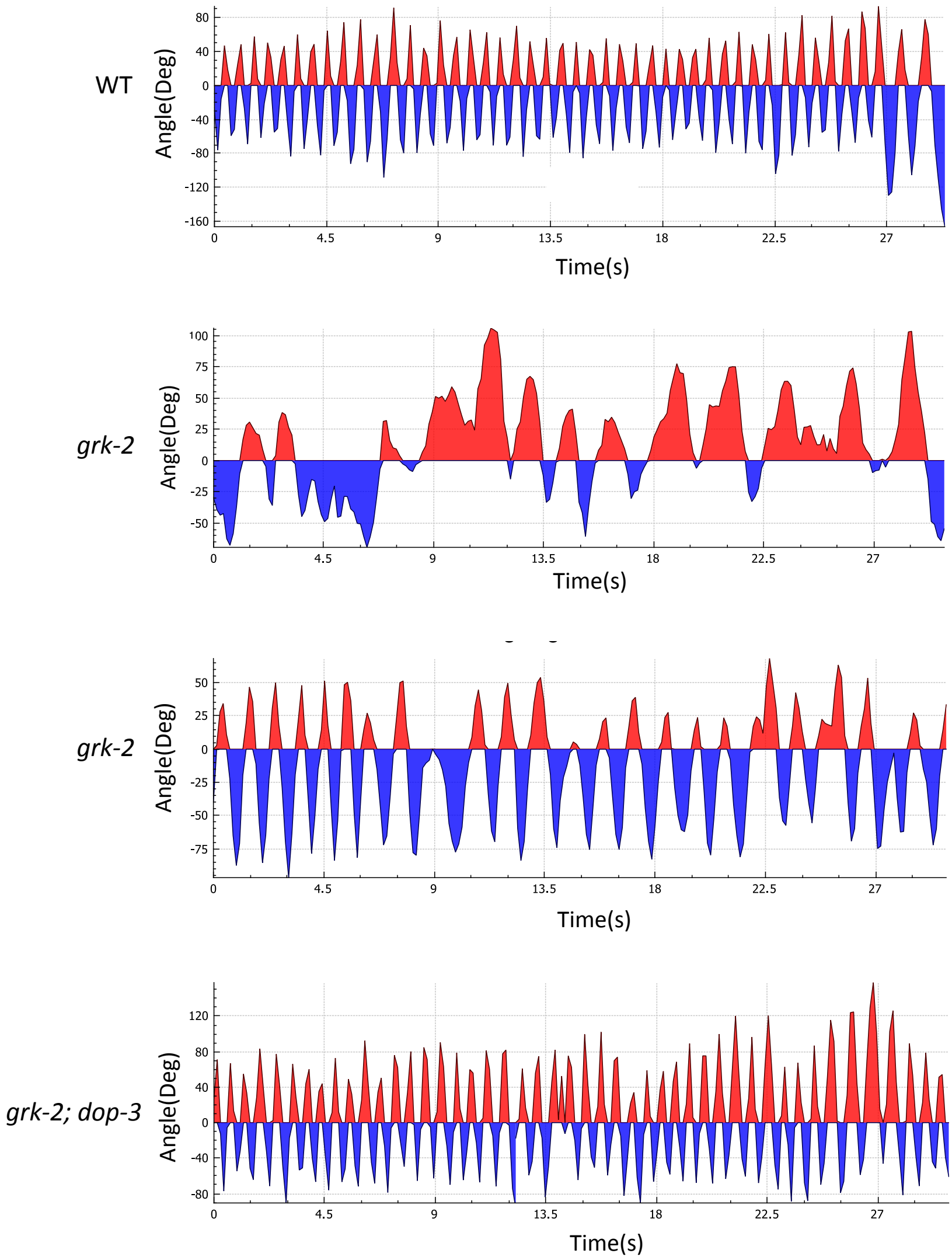
WT
Angle(Deg)
80
40
0
-40
-80
-120
-160
0
4.5
9
13.5
18
22.5
27
Time(s)
grk-2
Angle(Deg)
100
75
50
25
0
-25
-50
0
4.5
9
13.5
18
22.5
27
Time(s)
grk-2
Angle(Deg)
50
25
0
-25
-50
-75
0
4.5
9
13.5
18
22.5
27
Time(s)
grk-2; dop-3
Angle(Deg)
120
80
40
0
-40
-80
0
4.5
9
13.5
18
22.5
27
Time(s)

S3 Fig.

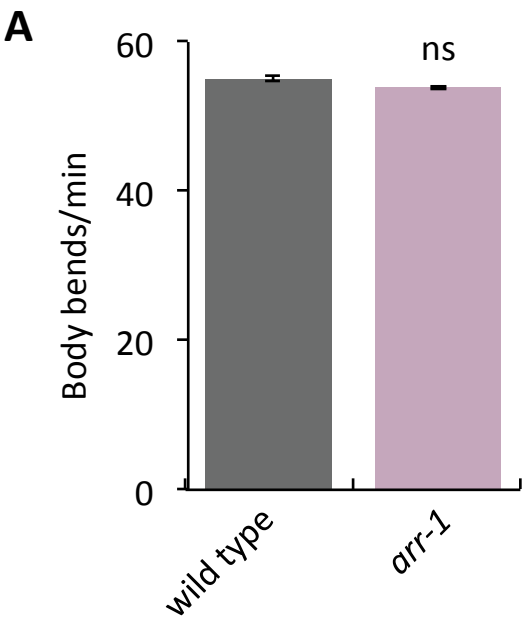
A
60
40
20
0
Body bends/min
ns
wild type
arr-1

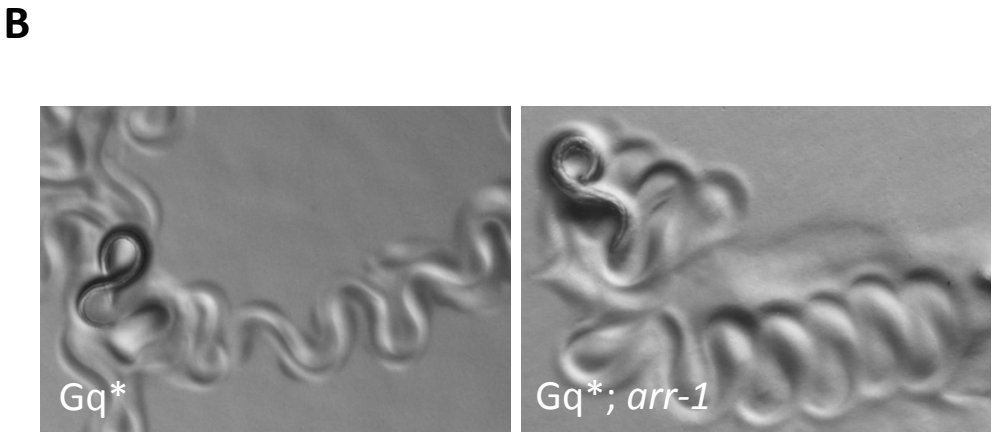
B
Gq*
Gq*; arr-1

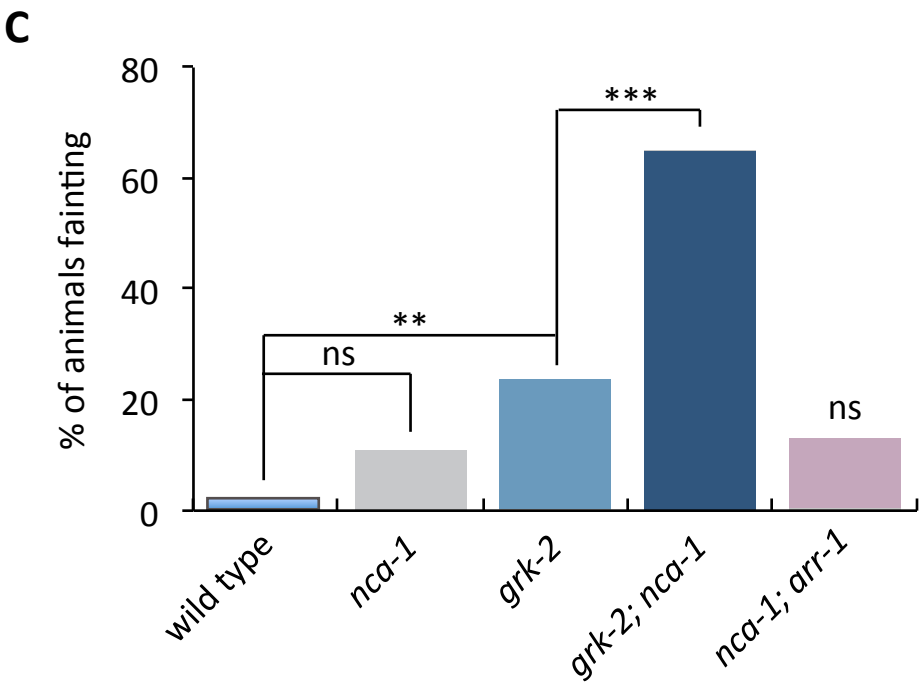
C
80
60
40
20
0
% of animals fainting
***
**
ns
ns
wild type
nca-1
grk-2
grk-2; nca-1
nca-1; arr-1

S4 Fig.

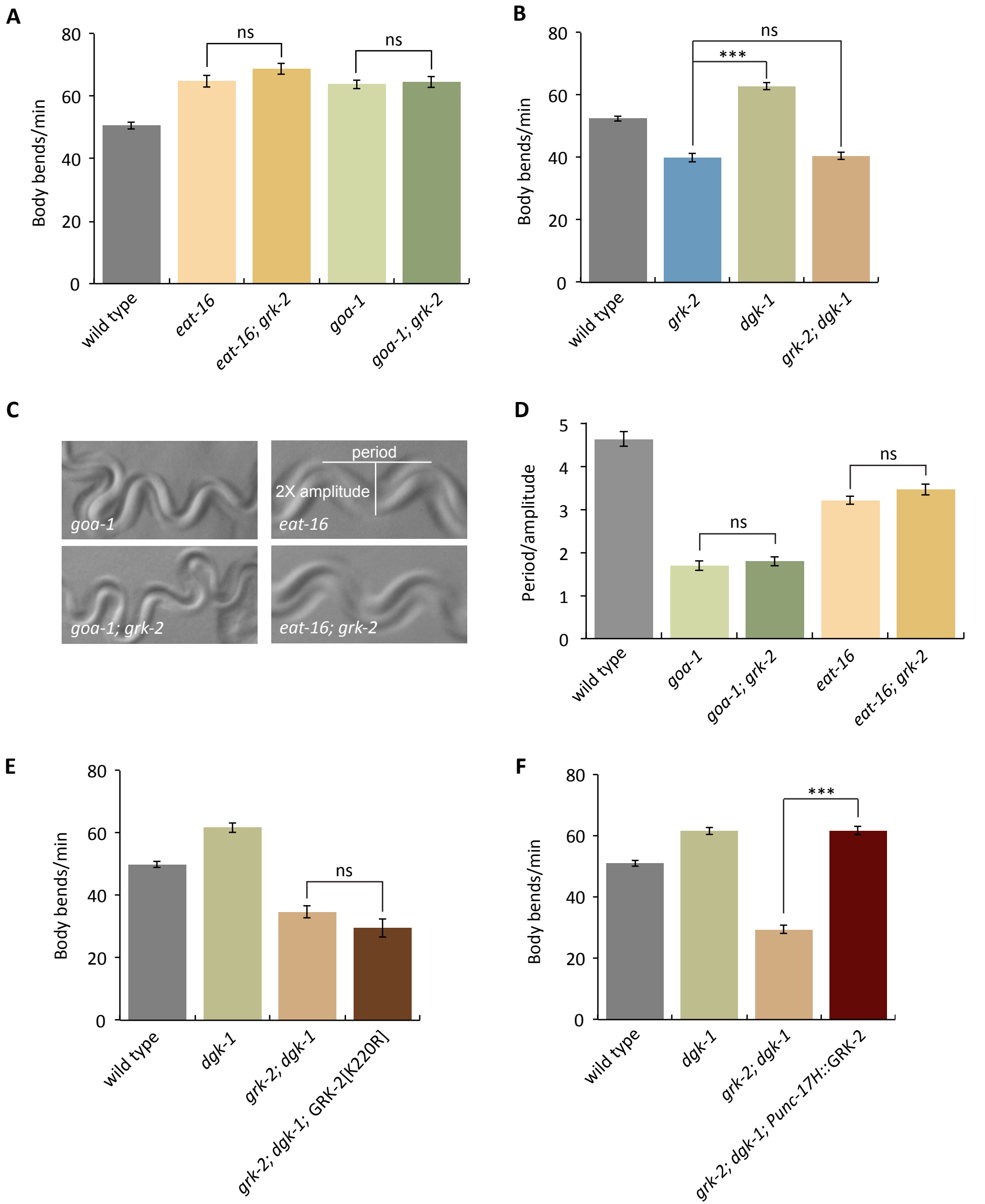
A
Body bends/min
80
60
40
20
0
ns
ns
wild type
eat-16
eat-16; grk-2
goa-1
goa-1; grk-2
B
Body bends/min
80
60
40
20
0
ns
***
wild type
grk-2
dgk-1
grk-2; dgk-1
C
goa-1
period
2X amplitude
eat-16
goa-1; grk-2
eat-16; grk-2
D
Period/amplitude
5
4
3
2
1
0
ns
ns
wild type
goa-1
goa-1; grk-2
eat-16
eat-16; grk-2
E
Body bends/min
80
60
40
20
0
ns
wild type
dgk-1
grk-2; dgk-1
grk-2; dgk-1; GRK-2[K220R]
F
Body bends/min
80
60
40
20
0
***
wild type
dgk-1
grk-2; dgk-1
grk-2; dgk-1; Punc-17H::GRK-2

S5 Fig

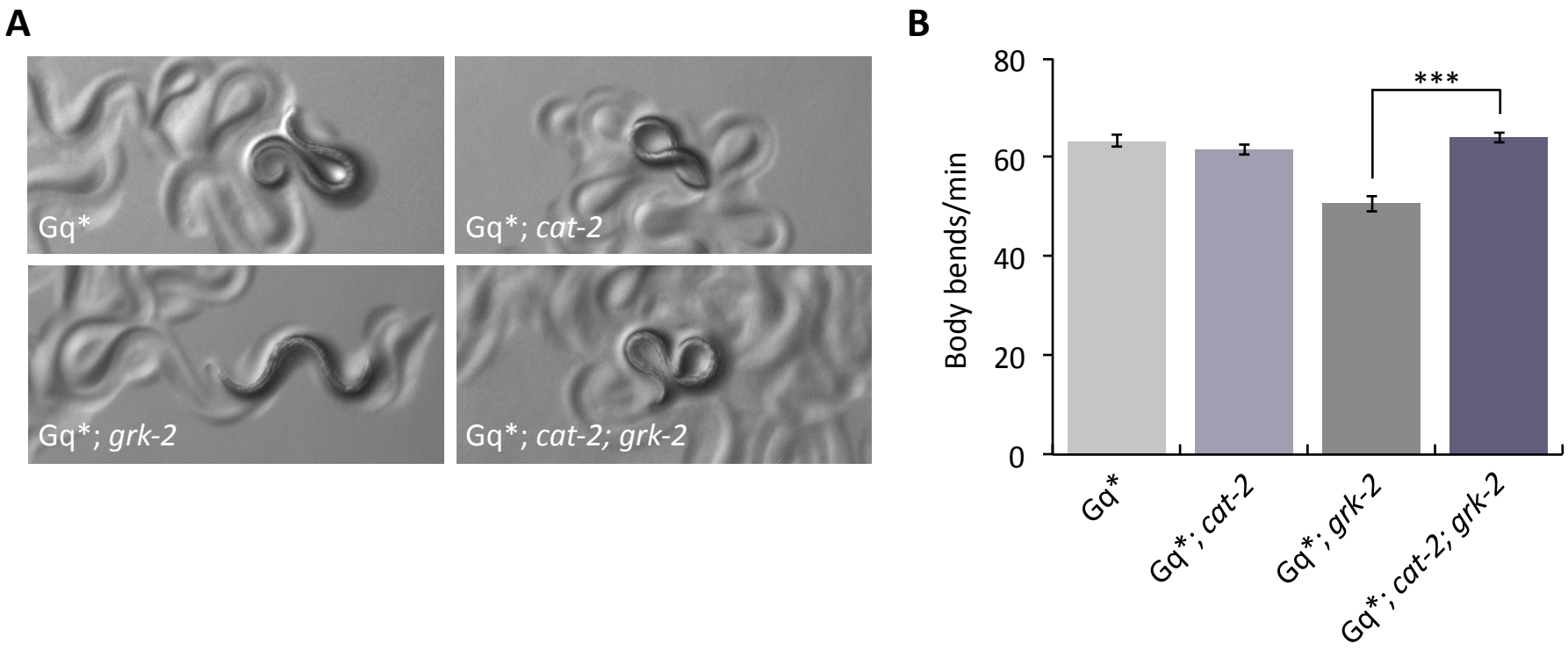
A
Gq*
Gq*; cat-2
Gq*; grk-2
Gq*; cat-2; grk-2
B
Body bends/min
80
60
40
20
0
***
Gq*
Gq*; cat-2
Gq*; grk-2
Gq*; cat-2; grk-2

S6 Fig.

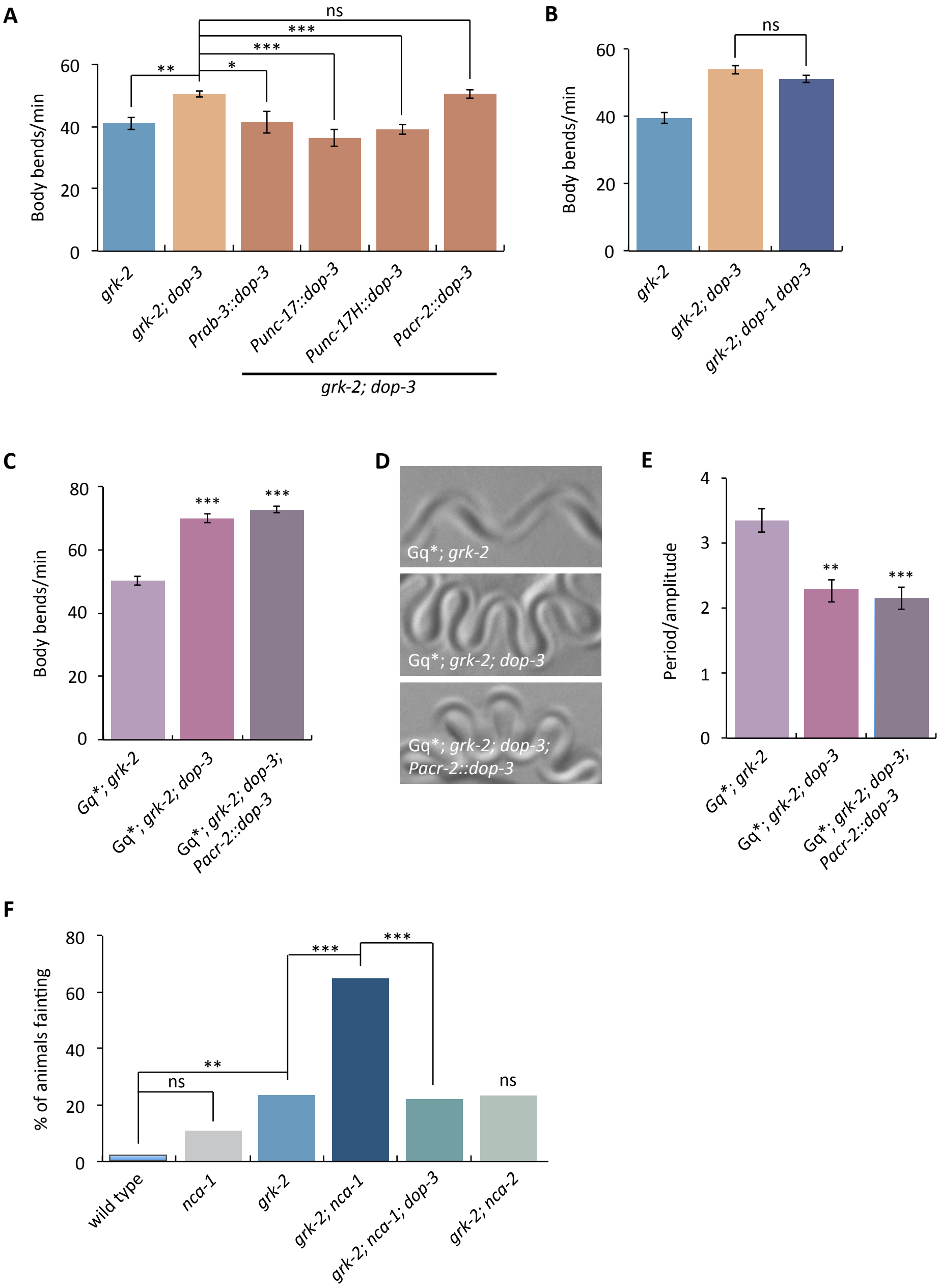
A
Body bends/min
60
40
20
0
ns
***
***
**
*
grk-2
grk-2; dop-3
Prab-3::dop-3
Punc-17::dop-3
Punc-17H::dop-3
Pacr-2::dop-3
grk-2; dop-3
B
Body bends/min
60
40
20
0
ns
grk-2
grk-2; dop-3
grk-2; dop-1 dop-3
C
Body bends/min
80
60
40
20
0
***
***
Gq*; grk-2
Gq*; grk-2; dop-3
Gq*; grk-2; dop-3; Pacr-2::dop-3
D
Gq*; grk-2
Gq*; grk-2; dop-3
Gq*; grk-2; dop-3; Pacr-2::dop-3
E
Period/amplitude
4
3
2
1
0
**
***
Gq*; grk-2
Gq*; grk-2; dop-3
Gq*; grk-2; dop-3; Pacr-2::dop-3
F
% of animals fainting
80
60
40
20
0
***
***
**
ns
ns
wild type
nca-1
grk-2
grk-2; nca-1
grk-2; nca-1; dop-3
grk-2; nca-2

S7 Fig

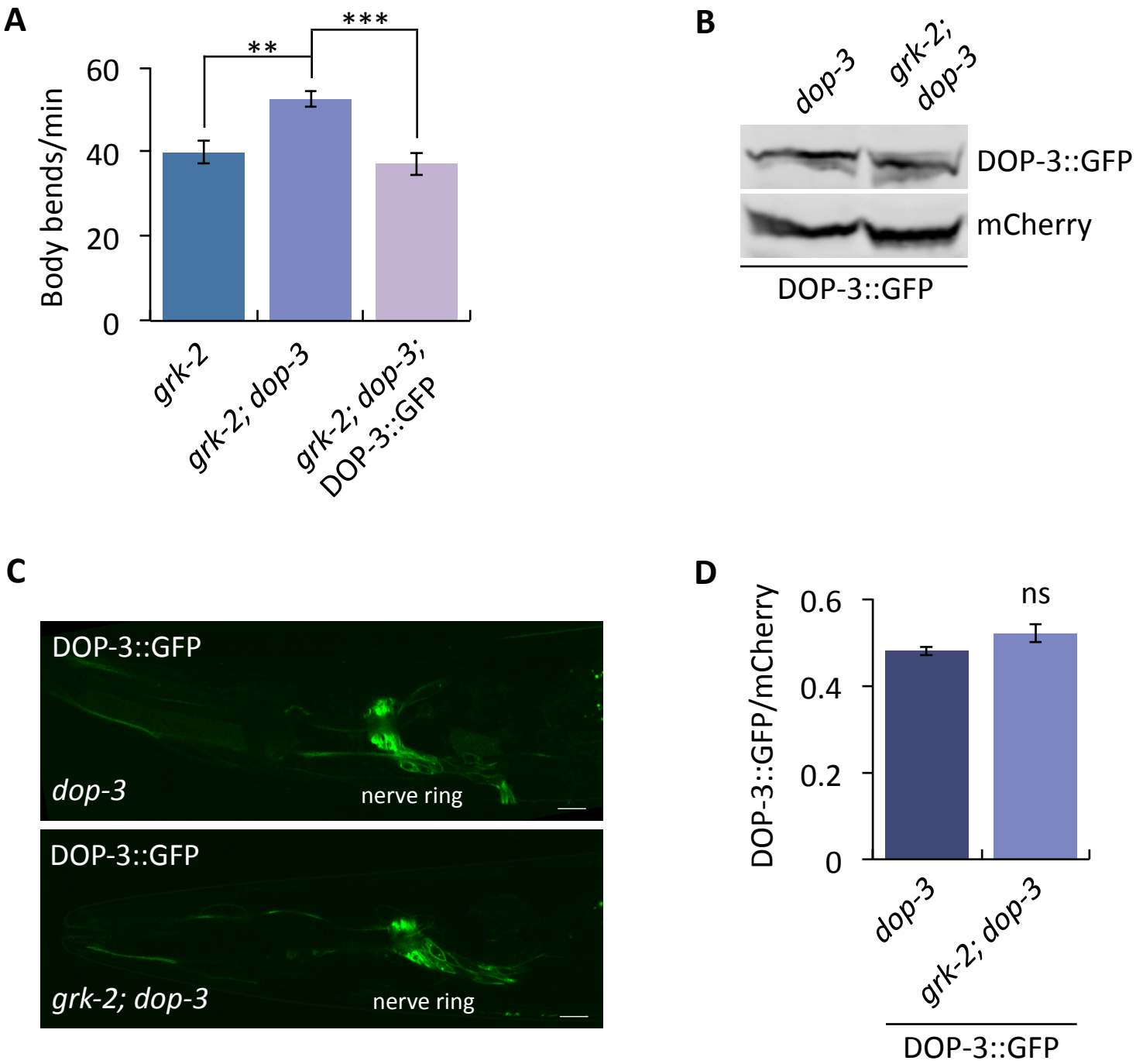
A
Body bends/min
60
40
20
0
**
***
grk-2
grk-2; dop-3
grk-2; dop-3; DOP-3::GFP
B
dop-3
grk-2; dop-3
DOP-3::GFP
mCherry
DOP-3::GFP
C
DOP-3::GFP
dop-3
nerve ring
DOP-3::GFP
grk-2; dop-3
nerve ring
D
DOP-3::GFP/mCherry
0.6
0.4
0.2
0
ns
dop-3
grk-2; dop-3
DOP-3::GFP

S8 Fig.

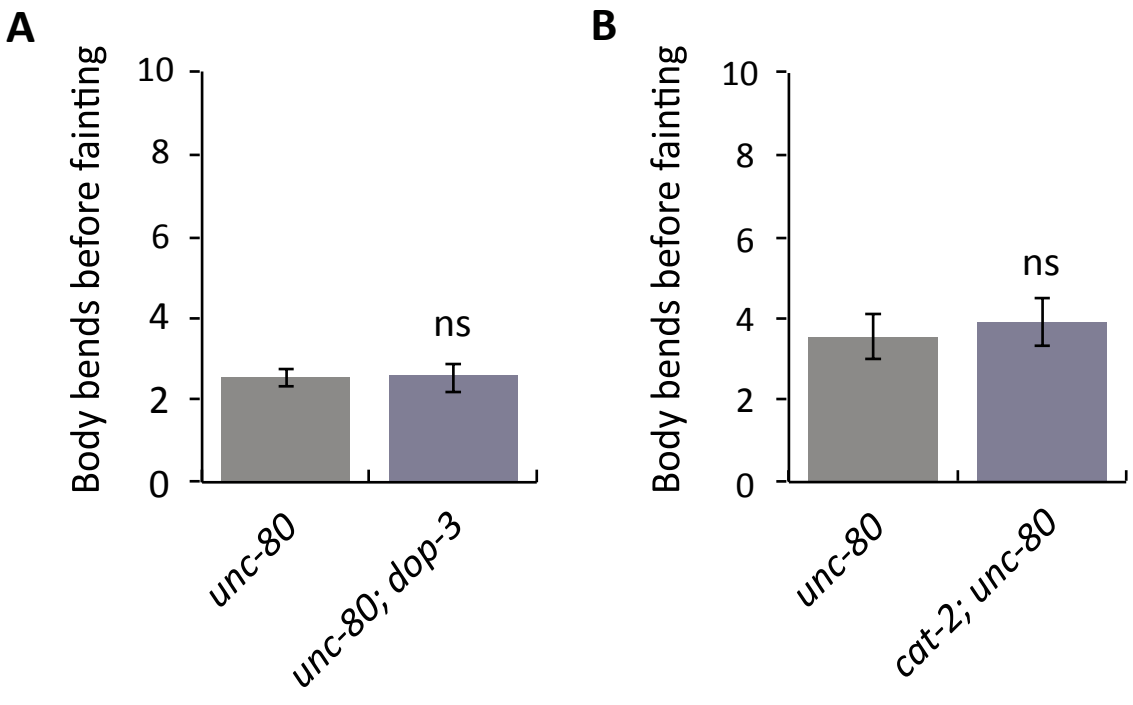
A
Body bends before fainting
10
8
6
4
2
0
ns
unc-80
unc-80; dop-3
B
Body bends before fainting
10
8
6
4
2
0
ns
unc-80
cat-2; unc-80

S9 Fig

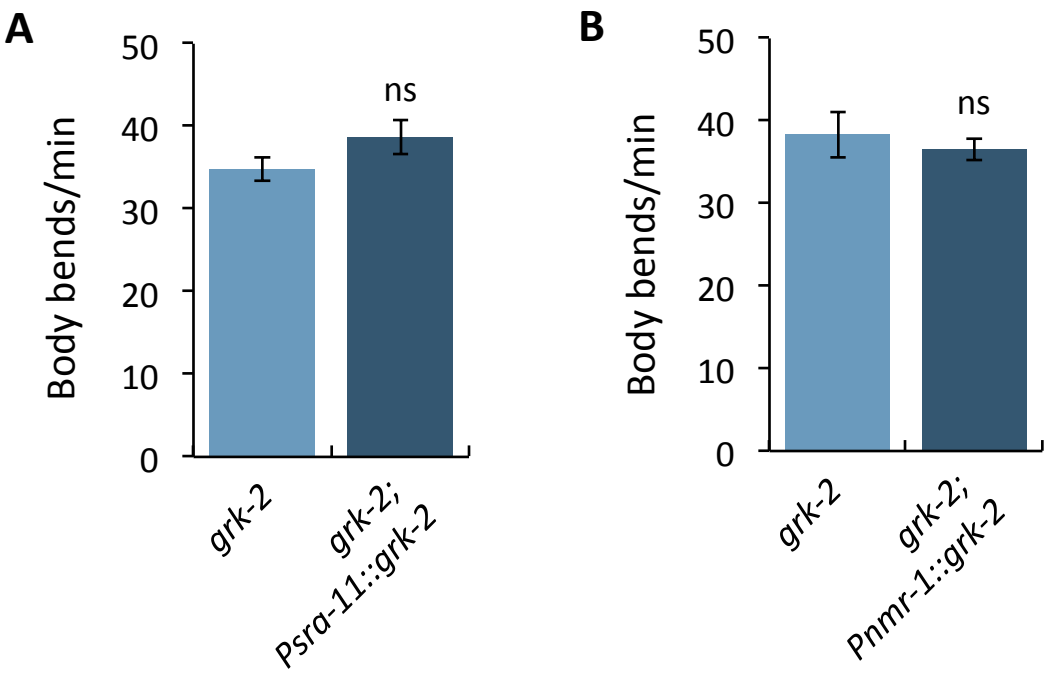
A
Body bends/min
50
40
30
20
10
0
ns
grk-2
grk-2;
Psra-11::grk-2
B
Body bends/min
50
40
30
20
10
0
ns
grk-2
grk-2;
Pnmr-1::grk-2

S1 Table. List of strains

N2: Bristol wild strain

CB1112: *cat-2(e1112) II*

CB4856: Hawaiian wild strain

EG317: *unc-73(ox317) I*

EG330: *unc-80(ox330) V*

EG352: *nca-1(ox352) IV*

EG4782: *nzIs29[Punc-17::rho-1(G14V), unc-122::gfp] II*

EG5504: *nlf-1(tm3631) X*

FG7: *grk-2(gk268) III*

JT47: *egl-8(sa47) V*

EG3745: *eat-16(tm775) I ; him-5(e1490) V*

JT734: *goa-1(sa734) I*

LX645: *dop-1(vs100) X*

LX703: *dop-3(vs106) X*

LX705: *dop-1(vs100) X dop-3(vs106) X*

MT8504: *egl-10(md176) V*

PS2627: *dgk-1(sy428) X*

RB660: *arr-1(ok401)* X

XZ1151: *egl-30(tg26) I*

The following strains were produced in this study:

XZ18: *grk-2(yak18) III*

XZ1089: *egl-30(tg26) I ; grk-2(yak18) III*

XZ1527: *egl-30(tg26) I ; grk-2(gk268) III*

XZ1531: *grk-2(gk268) III ; egl-8(sa47) V*

XZ1532: *unc-73(ox317) I ; grk-2(gk268) III*

XZ1544: *grk-2(gk268) III ; yakEx44[Prab-3::grk-2 cDNA::tbb-2 3'UTR::OPERON::GFP::H2B, Pmyo-3::mCherry]*

XZ1549: *grk-2(gk268) III ; yakEx45[Punc-17::grk-2 cDNA::tbb-2 3'UTR::OPERON::GFP::H2B, Pmyo-2::mCherry]*

XZ1551: *grk-2(gk268) III ; yakEx47[Pacr-2::grk-2 cDNA::tbb-2 3'UTR::OPERON::GFP::H2B, Pmyo-2::mCherry]*

XZ1552: *grk-2(gk268) III ; yakEx48[GRK-2[K220R], Pmyo-2::mCherry]*

XZ1559: *nzIs29[Punc-17::rho-1(G14V), unc-122::gfp] II ; grk-2(gk268) III*

XZ1560: *grk-2(gk268) III ; nca-1(ox352) IV*

XZ1561: *grk-2(gk268) III ; yakEx51[Punc-17H::grk-2 cDNA::tbb-2 3'UTR::OPERON::GFP::H2B, Pmyo-3::mCherry]*

XZ1562: *grk-2(gk268) III ; yakEx52[Pglr-1::grk-2 cDNA::tbb-2 3'UTR::OPERON::GFP::H2B, Pmyo-2::mCherry]*

XZ1563: *grk-2(gk268) III ; yakEx53[Posm-6::grk-2 cDNA::tbb-2 3'UTR::OPERON::GFP::H2B, Pmyo-3::mCherry]*

XZ1571: *grk-2(gk268) III ; yakEx54[Pgrk-2::grk-2 cDNA::tagRFP, Pmyo-3::GFP]*

XZ1579: *grk-2(gk268) III ; yakEx55[GRK-2[Y109I], Pmyo-2::mCherry]*

XZ1581: *grk-2(gk268) III ; dgk-1(sy428) X*

XZ1582: *grk-2(gk268) III ; yakEx57[GRK-2[R106A], Pmyo-2::mCherry]*

XZ1583: *grk-2(gk268) III ; yakEx56[GRK-2[D110A], Pmyo-2::mCherry]*

XZ1641: *grk-2(gk268) III ; yakEx71[Pxbx-1::grk-2 cDNA::tbb-2 3'UTR::OPERON::GFP::H2B, Pmyo-2::mCherry]*

XZ1675: *grk-2(gk268) III ; yakEx77[GRK-2[D3K], Pmyo-2:mCherry]*

XZ1676: *grk-2(gk268) III ; yakEx78[GRK-2[L4K], Pmyo-2:mCherry]*

XZ1684: *eat-16(tm775) I ; grk-2(gk268) III*

XZ1691: *grk-2(gk268) III ; nlf-1(tm3631) X*

XZ1692: *grk-2(gk268) III ; yakEx79[GRK-2[V7A/L8A], Pmyo-2:mCherry]*

XZ1693: *grk-2(gk268) III ; yakEx80[GRK-2[D10A], Pmyo-2:mCherry]*

XZ1694: *grk-2(gk268) III ; dgk-1(sy428) X ; yakEx51[Punc-17H::grk-2 cDNA::tbb-2 3'UTR::OPERON::GFP::H2B,*

Pmyo-3::mCherry]

XZ1695: *grk-2(gk268) III ; dgk-1(sy428) X ; yakEx48[GRK-2[K220R], Pmyo-2::mCherry]*

XZ1713: *goa-1(sa734) I ; grk-2(gk268) III*

XZ1724: *grk-2(gk268) III ; yakEx85[Pnmr-1::grk-2cDNA::tbb-2 3'UTR::OPERON:GFP::H2B, Pmyo-2::mCherry]*

XZ1727: *grk-2(gk268) III ; yakEx87[GRK-2[K567E], Pmyo-2::mCherry]*

XZ1728: *grk-2(gk268) III ; yakEx88[GRK-2[R587Q], Pmyo-2::mCherry]*

XZ1729 *grk-2(gk268) III ; nca-1(gk9) IV*

XZ1730 *grk-2(gk268) III ; nca-2(gk5) III*

XZ1766: *grk-2(gk268) III ; yakEx95[GRK-2[R195A], Pmyo-2::mCherry]*

XZ1767: *grk-2(gk268) III ; yakIs19[Pgrk-2::grk-2 cDNA::tagRFP] ; yakEx94[Punc-17H::eGFP::let-858 3'UTR]*

XZ1845: *yakEx103[Punc-17H::GOA-1[Q205L]::tbb-2 3'UTR::OPERON::GFP::H2B, Pmyo-2::mCherry]*

XZ1859: *egl-10(md176) V ; nlf-1(tm3631) X*

XZ1876: *nlf-1(tm3631) X ; yakEx103[Punc-17H::GOA-1[Q205L]::tbb-2 3'UTR::OPERON::GFP::H2B, Pmyo-2::mCherry]*

XZ1903: *grk-2(gk268) III ; dop-3(vs106) X*

XZ1904: *egl-30(tg26) I ; grk-2(gk268) III ; dop-3(vs106) X*

XZ1905: *cat-2(e1112) II ; grk-2(gk268) III*

XZ1906: *egl-30(tg26) I ; cat-2(e1112) II ; grk-2(gk268) III*

XZ1909: *grk-2(gk268) III ; dop-3(vs106) X ; yakEx109[Pacr-2::dop-3 cDNA::tbb-2 3'UTR::OPERON::GFP::H2B, Pmyo-2::mCherry]*

XZ1910: *grk-2(gk268) III ; dop-3(vs106) X ; yakEx110[Punc-17H::dop-3 cDNA::tbb-2 3'UTR::OPERON::GFP::H2B, Pmyo-2::mCherry]*

XZ1911: *grk-2(gk268) III ; dop-3(vs106) X ; yakEx111[Punc-17::dop-3 cDNA::tbb-2 3'UTR::OPERON::GFP::H2B, Pmyo-2::mCherry]*

XZ1912: *grk-2(gk268) III ; dop-3(vs106) X ; yakEx112[Prab-3::dop-3 cDNA::tbb-2 3'UTR::OPERON::GFP::H2B,*

Pmyo-2::mCherry]

XZ1925: *cat-2(e1112) II ; unc-80(ox330) V*

XZ1935: *cat-2(e1112) II ; nlf-1(tm3631) X*

XZ1936: *unc-80(ox330) V ; dop-3(vs106) X*

XZ1940: *nlf-1(tm3631) X dop-3(vs106) X*

XZ1941: *grk-2(gk268) III ; nlf-1(tm3631) X dop-3(vs106) X*

XZ2007: *grk-2(gk268) III ; dop-1(vs100) X dop-3(vs106) X*

XZ2028: *egl-30(tg26) I ; grk-2(gk268) III ; yakEx48[GRK-2(K220R), Pmyo-2::mCherry]*

XZ2029: *egl-30(tg26) I ; grk-2(gk268) III ; yakEx51[Punc-17H::grk-2 cDNA::tbb-2 3'UTR::OPERON::GFP::H2B, Pmyo-3::mCherry]*

XZ2063: *dop-3(vs106) X ; yakEx130[Pgrk-2::dop-3 cDNA::GFP, Pmyo-2::mCherry]*

XZ2066: *nca-1(gk9) IV ; arr-1(ok401) X*

XZ2071: *grk-2(gk268) III ; yakEx135[Pcho-1(3.3 to 2.6)::grk-2 cDNA::tbb-2 3'UTR::OPERON::GFP::H2B, Pmyo-2::mCherry]*

XZ2075 *grk-2(gk268) III ; yakEx138[Pttx-3::grk-2 cDNA::tbb-2 3'UTR::OPERON::GFP::H2B, Pmyo-2::mCherry]*

XZ2078 *grk-2(gk268) III ; yakEx141[Psra-11::grk-2 cDNA::tbb-2 3'UTR::OPERON::GFP::H2B, Pnmr-1::grk-2 cDNA:: tbb-2 3'UTR::OPERON::GFP::H2B, Pmyo-2::mCherry]*

XZ2086 *grk-2(gk268) III ; yakEx147[Psra-11::grk-2 cDNA::tbb-2 3'UTR::OPERON::GFP::H2B, Pmyo-2::mCherry]*

XZ2087 *grk-2(gk268) III ; dop-3(vs106) X ; yakEx148[Psra-11::dop-3 cDNA::tbb-2 3'UTR::OPERON::GFP::H2B, Pnmr-1::dop-3 cDNA::tbb-2 3'UTR::OPERON::GFP::H2B, Pmyo-2::mCherry]*

XZ2088 *grk-2(gk268) III ; nlf-1(tm3631) X ; yakEx141[Psra-11::grk-2 cDNA::tbb-2 3'UTR::OPERON::GFP::H2B, Pnmr-1::grk-2 cDNA:: tbb-2 3'UTR::OPERON::GFP::H2B, Pmyo-2::mCherry]*

XZ2089: *grk-2(gk268) III ; yakEx149[Pceh-24::grk-2 cDNA::tbb-2 3'UTR::OPERON::GFP::H2B, Pmyo-2::mCherry]*

XZ2090: *grk-2(gk268) III ; dop-3(vs106) X ; yakEx130[Pgrk-2::dop-3 cDNA::GFP, Pmyo-2::mCherry]*

XZ2091: *egl-30(tg26) I ; grk-2(gk268) III ; dop-3(vs106) X ; yakEx109[Pacr-2::dop-3 cDNA::tbb-2 3'UTR::OPERON::GFP::H2B, Pmyo-2::mCherry]*

XZ2095: *otIs534[Pcho-1^{fosmid}::SL2::YFP::H2B] ; yakIs19[Pgrk-2::grk-2 cDNA::tagRFP]*

S2 Table. List of plasmids

Gateway destination vectors

pCFJ150	Gateway destination vector for insertion at chr II Mos site *ttTi5605*

Gateway entry clones

GL29	*Psra-11* [4-1] (4922 bp of the *sra-11* promoter upstream of the ATG)
pADA180	*Punc-17H* [4-1] (derived from the *unc-17* promoter of pGH1, carrying a 127 bp deletion that removes the nerve cord β enhancer, expressed in head acetylcholine neurons)
p_C06E1.4_93	*Pglr-1* [4-1] (from Open Biosystems) (727 bp of the *glr-1* promoter upstream of and including the ATG)
pCFJ31	*Pacr-2* [4-1] (3362 bp of the *acr-2* promoter upstream of the ATG)
pCFJ326	*tbb-2 3'UTR*::OPERON::GFP::H2B [2-3]
pCR185	GFP::*unc-54* 3'UTR [2-3]
pEGB05	*Prab-3* [4-1] (1210 bp of the *rab-3* promoter upstream of the ATG)
pET68	*grk-2* cDNA [1-2]
pET85	*Posm-6* [4-1] (2400 bp of the *osm-6* promoter upstream of the ATG)
pET89	*Pgrk-2* [4-1] (2895 bp of the *grk-2* promoter upstream of the ATG)
pET108	*Pxbx-1* [4-1] (373 bp of the *xbx-1* promoter upstream of the ATG)
pET134	*goa-1*[Q205L] cDNA [1-2]
pET139	*dop-3* cDNA with stop codon [1-2]
pET181	*dop-3* cDNA without stop codon [1-2]

pET185	*Pcho-1*(3.3-2.6) [4-1] (fragment of the *cho-1* promoter from 3300 bp to 2600 bp upstream of the ATG)
pET186	*Pceh-24* [4-1] (3013 bp of the *ceh-24* promoter upstream of the ATG)
pET196	*Pttx-3* [4-1] (414 bp fragment of the *ttx-3* genomic region starting from the second exon and including the AIY motif that directs expression only in AIY)
pGH1	*Punc-17* [4-1] (3229 bp of the *unc-17* promoter upstream of and including the ATG)
pGH107	tagRFP::*let-858* 3'UTR [2-3]
pMA102	*Pnmr-1* [4-1] (4709 bp of the *nmr-1* promoter upstream of the ATG)

<u>Gateway expression constructs</u>

pET79	*Prab-3::grk-2 cDNA::tbb-2 3'UTR*::OPERON::GFP::H2B_pCFJ150
pET81	*Punc-17::grk-2 cDNA::tbb-2 3'UTR:*:OPERON::GFP::H2B_pCFJ150
pET82	*Punc-17H::grk-2 cDNA::tbb-2 3'UTR*::OPERON::GFP::H2B_pCFJ150
pET83	*Pacr-2::grk-2 cDNA::tbb-2 3'UTR*::OPERON::GFP::H2B_pCFJ150
pET86	*Posm-6::grk-2 cDNA::tbb-2 3'UTR*::OPERON::GFP::H2B_pCFJ150
pET88	*Pglr-1::grk-2 cDNA::tbb-2 3'UTR*::OPERON::GFP::H2B_pCFJ150
pET90	*Pgrk-2::grk-2 cDNA*::GFP_pCFJ150
pET91	*Pgrk-2::grk-2 cDNA*::tagRFP_pCFJ150
pET93	*Punc-17H::eGFP::let-858 3'UTR*_pCFJ150
pET109	*Pxbx-1::grk-2 cDNA::tbb-2 3'UTR*::OPERON::GFP::H2B_pCFJ150

pET119 *Pnmr-1::grk-2 cDNA::tbb-2 3'UTR*::OPERON::GFP::H2B_pCFJ150

pET135 *Punc-17H::GOA-1[Q205L]::tbb-2 3'UTR*::OPERON::GFP::H2B_pCFJ150

pET140 *Prab-3::dop-3 cDNA::tbb-2 3'UTR*::OPERON::GFP::H2B_pCFJ150

pET141 *Pacr-2::dop-3 cDNA::tbb-2 3'UTR*::OPERON::GFP::H2B_pCFJ150

pET142 *Punc-17::dop-3 cDNA::tbb-2 3'UTR*::OPERON::GFP::H2B_pCFJ150

pET143 *Punc-17H::dop-3 cDNA::tbb-2 3'UTR*::OPERON::GFP::H2B_pCFJ150

pET184 *Pgrk-2::dop-3 cDNA*::GFP_pCFJ150

pET190 *Pceh-24::grk-2 cDNA::tbb-2 3'UTR*::OPERON::GFP::H2B_pCFJ150

pET191 *Pcho-1(3.3-2.6)::grk-2 cDNA::tbb-2 3'UTR*::OPERON::GFP::H2B_pCFJ150

pET197 *Pttx-3::grk-2 cDNA::tbb-2* 3'UTR::OPERON-GFP::H2B_pCFJ150

pET209 *Pnmr-1::dop-3 cDNA::tbb-2 3'UTR*::OPERON::GFP::H2B_pCFJ150

pET214 *Psra-11::grk-2 cDNA::tbb-2 3'UTR*::OPERON::GFP::H2B_pCFJ150

pET215 *Psra-11::dop-3 cDNA::tbb-2 3'UTR*::OPERON::GFP::H2B_pCFJ150

Plasmids used for the GRK-2 structure-function analysis: from Wood et al., 2012.

pFG45 *Pgrk-2::*GRK-2

pFG46 *Pgrk-2::*GRK-2[D3K]

pFG47 *Pgrk-2::*GRK-2[L4K]

pFG48 *Pgrk-2::*GRK-2[V7A/L8A]

pFG49 *Pgrk-2::*GRK-2[D10A]

pFG84 *Pgrk-2::*GRK-2[R195A]

pFG85 *Pgrk-2::*GRK-2[R106A]

pFG86	*Pgrk-2::*GRK-2[Y109I]
pFG87	*Pgrk-2::*GRK-2[D110A]
pFG88	*Pgrk-2::*GRK-2[K220R]
pFG89	*Pgrk-2::*GRK-2[K567E]
pFG90	*Pgrk-2::*GRK-2[R587Q]